OPEN

Genotype-Phenotype Correlation Study in a Large Series of Patients Carrying the p.Pro51Ser (p.P51S) Variant in *COCH* (DFNA9) Part II: A Prospective Cross-Sectional Study of the Vestibular Phenotype in 111 Carriers

Sebastien P. F. JanssensdeVarebeke,[1,2] Julie Moyaert,[3] Erik Fransen,[4,5] Britt Bulen,[1] Celine Neesen,[1] Katrien Devroye,[1] Raymond van de Berg,[6] Ronald J. E. Pennings,[7,8] Vedat Topsakal,[3] Olivier Vanderveken,[3] Guy Van Camp,[4,9] and Vincent Van Rompaey[2,3]

Introduction: DFNA9 is characterized by adult-onset hearing loss and evolution toward bilateral vestibulopathy (BVP). The genotype-phenotype correlation studies were conducted 15 years ago. However, their conclusions were mainly based on symptomatic carriers and the vestibular data exclusively derived from the horizontal (lateral) semicircular canal (SCC). The last decade was marked by the emergence of new clinical diagnostic tools, such as the video head impulse test (vHIT) and vestibular-evoked myogenic evoked potentials (VEMPs), expanding our evaluation to all six SCCs and the otolith organs (saccule and utricule).

Aim: The aim of this study was to comprehensively evaluate vestibular function in the largest series presymptomatic as well as symptomatic p.P51S variant carriers, to determine which labyrinthine part shows the first signs of deterioration and which SCC function declines at first and to determine the age at which p.P51S variant carriers develop caloric areflexia on VNG and vHIT vestibulo-ocular reflex (VOR)-gain dysfunction as defined by the Barany Society criteria for BVP.

Material and methods: One hundred eleven p.P51S variant carriers were included. The following vestibular function tests were applied in two different centers: ENG/VNG, vHIT, and VEMPs. The following parameters were analyzed: age (years), hearing loss (pure-tone average of 0.5–4 kHz [$PTA^{0.5-4}$, dB HL]), sum of maximal peak slow-phase eye velocity obtained with bi-thermal (30°C and 44°C, water irrigation; 25°C and 44°C, air irrigation) caloric test (°/s), vHIT VOR-gain on LSCC, superior SCC and posterior SCC, C-VEMP both numerical (threshold, dB nHL) and categorical (present or absent), and O-VEMP as categorical (present or absent). The age of onset of vestibular dysfunction was determined both with categorical (onset in decades using Box & Whisker plots) and numeric approach (onset in years using regression analysis). The same method was applied for determining the age at which vestibular function declined beyond the limits of BVP, as defined by the Barany Society.

Results: With the categorical approach, otolith function was declining first (3rd decade), followed by caloric response (5th decade) and vHIT VOR-gains (5th–6th decade). Estimated age of onset showed that the deterioration began with C-VEMP activity (31 years), followed by caloric responses (water irrigation) (35 years) and ended with vHIT VOR-gains (48–57 years). Hearing deterioration started earlier than vestibular deterioration in female carriers, which is different from earlier reports. BVP was predicted at about 53 years of age on average with VNG caloric gain (water irrigation) and between 47 and 57 years of age for the three SCCs. Loss of C-VEMP response was estimated at about 46 years of age.

Conclusion: Former hypothesis of vestibular decline preceding hearing deterioration by 9 years was confirmed by the numeric approach, but this was less obvious with the categorical approach. Wide confidence intervals of the regression models may explain deviation of the fits from true relationship. There is a typical vestibular deterioration hierarchy in p.P51S variant carriers. To further refine the present findings, a prospective longitudinal study of the auditory and vestibular phenotype may help to get even better insights in this matter.

Key words: Bilateral vestibulopathy, DFNA9, Human COCH protein, Progressive vestibulocochlear dysfunction, Sensorineural hearing loss, Vestibulo-ocular reflex.

Abbreviations: ARTV = age-related typical vestibulograms; ARTvH = age-related typical video HITs; BVP = bilateral vestibulopathy; COCH = coagulation factor C homology; ED = effective dose; ENG = electronystagmography; LARP = left anterior right posterior; LCCL = Limulus clotting factor C, Cochlin; LL/RL = left lateral/right lateral; LSCC = lateral semicircular canal; p.P51S: c.151C>T = pPro51Ser; PSCC = posterior semicircular canal; PTA = pure-tone average; RALP = right anterior left posterior; SCC = semicircular canal; SCM = sternocleidomastoid muscle; SNHL = sensorineural hearing loss; SPV = slow-phase velocity; SSCC = superior semicircular canal; VEMP = vestibular-evoked myogenic evoked potentials; vHIT = the video Head Impulse Test; VNG = videonystagmography; VOR = vestibulo-ocular reflex; vWFA 2 = von Willebrand Factor-like domain type 2.

(Ear & Hearing 2021;42;1525–1543)

INTRODUCTION AND AIM OF THE STUDY

Bilateral vestibulopathy (BVP) is a chronic vestibular syndrome characterized by a bilaterally absent or partially reduced vestibular function (Strupp et al. 2017). The leading symptoms of BVP are oscillopsia, postural imbalance, and gait unsteadiness

[1]Department of Otorhinolaryngology—Head & Neck Surgery, Jessa Hospital, Hasselt, Belgium; [2]Department of Translational Neurosciences, Faculty of Medicine and Health Sciences, University of Antwerp, Belgium; [3]Department of ENT HNS, University Hospital Brussels, Belgium; [4]Center of Medical Genetics, University of Antwerp, Belgium; [5]StatUa, University of Antwerp, Belgium; [6]Department of Otorhinolaryngology Head & Neck Surgery, Medisch Universitair Medisch Centrum (MUMC), Maastricht, The Netherlands; [7]Hearing and Genes, Department of Otorhinolaryngology—Head and Neck Surgery, Radboud University Medical Center, Nijmegen, The Netherlands; [8]Donders Institute for Brain, Cognition and Behaviour, Radboud University Medical Center, Nijmegen, The Netherlands; and [9]Department of Medical Genetics, Antwerp University Hospital, Belgium.

Supplemental digital content is available for this article. Direct URL citations appear in the printed text and are provided in the HTML and text of this article on the journal's Web site (www.ear-hearing.com).

<zdoi; 10.1097/AUD.0000000000001070>

exacerbated by visual deprivation or when walking on uneven ground (Strupp et al. 2017; Dobbels et al. 2019; Lucieer et al. 2020). Oscillopsia is caused by impairment of the vestibulo-ocular reflex (VOR), which is essential for gaze stabilization (Hermann et al. 2018). Not only BVP has an impact on health-related quality of life and cognitive functioning, it also leads to an increased risk of falling and severe fall-related injuries (Guinand et al. 2012; Sun et al. 2014; Hermann et al. 2018; Agrawal et al. 2018). For example, 39% of BVP patients reported at least one fall-event in the last year. Among the etiologies of BVP are ototoxicity due to aminoglycosides, bilateral Menière's disease, meningitis, neurofibromatosis type 2, cholesteatoma, iatrogenic damage due to surgery, autoimmune and hereditary disorders affecting the inner ear, such as Cogan's syndrome, etc. (Rinne et al. 1998; Zingler et al. 2007; Kim et al. 2011; Lucieer et al. 2016). Approximately 50% of the cause remain unknown (Rinne et al. 1998; Zingler et al. 2007; Kim et al. 2011; Lucieer et al. 2016).

However, peripheral vestibular disorders can also have a genetic origin, which either can be isolated, or in association with hearing loss, such as for instance DFNA9, DFNA11, DFNA15, DFNA28, enlarged vestibular aqueduct syndrome, and Usher syndrome (Eppsteiner & Smith 2011). Many of these Mendelian hearing losses are associated with late-onset hearing and vestibular deterioration (Eppsteiner & Smith 2011).

DFNA9 is an autosomal dominantly inherited inner ear disease caused by mutations in *COCH* (coagulation factor C Homology) (Manolis et al. 1996; Robertson et al. 1997, 2001).

It is the ninth locus that has been associated with autosomal dominant hearing loss, and it is characterized by adult-onset sensorineural hearing loss (SNHL) and evolution towards BVP. It was first described by Verhagen et al. (1988), The Netherlands. It was linked to chromosome 14q12-13 in 1992 and located in the *COCH* gene in 1996 (Robertson et al. 1994; Manolis et al. 1996; Robertson et al. 1998; Fransen & Van Camp 1999; Robertson et al. 2001).

The *COCH* gene encodes for cochlin protein, which represents 80% of all cochlear proteins (Ikezono et al. 2001; Robertson et al. 2003). Eosinophilic deposits of misfolded mutant cochlin have been described at the same inner ear sites where *COCH* shows the highest expression, which is the cochlear spiral limbus, spiral ligament, and osseous spiral lamina as well as the crista ampullaris of vestibular semicircular canals (SCCs) (Khetarpal 2000).

To date, 31 different mutations have been described in *COCH* worldwide and newly discovered variants are published every year (Downie et al. 2020). The vestibular impairment depends on the molecular location of the mutation in *COCH* (Bae et al. 2014). Those located more upstream in the Limulus clotting factor C, Cochlin (LCCL) domain are associated with late-onset hearing loss (4th decade). These variants also cause more pronounced vestibular signs due to the misfolding of mutant cochlin, which accumulates in the extracellular matrix (deposits) and eventually cause secondary degeneration of dendritic neural cells. In opposition, the more downstream located mutations, for instance the von Willebrand Factor-like domains type 2 (vWFA2), express with early-onset hearing deterioration (2nd decade). Most of these variants have limited or complete absence of vestibular symptoms, because mutant cochlin accumulates intracellularly and leads to early cell death (Bae et al. 2014). All mutations in *COCH* have autosomal dominant inheritance, except for two autosomal recessive loss-of-function mutations causing congenital hearing deterioration without apparent vestibular loss (at young ages, according to current data) (JanssensdeVarebeke et al. 2018; Downie et al. 2020; Booth et al. 2020).

The auditory phenotype of the c.151C>T, pPro51Ser (p.P51S) variant is characterized with an adult-onset progressive, sensorineural, asymmetric hearing deterioration, which typically starts at the high frequencies around 27 years of age, with an averaged decline of about 2.8 dB/year across all frequencies. Carriers are potentially eligible for hearing aids at an average age of 46, while they become candidates for cochlear implantation at an average age of 59, as we described in part I of this two-part prospective cross-sectional study.

The genotype-phenotype correlation studies of this variant were conducted 15 years ago (de Kok et al. 1999; Bom et al. 1999, 2003; Bischoff et al. 2005). However, their conclusions were based on data derived from mainly symptomatic carriers. Moreover, the vestibular data were exclusively derived from the horizontal (lateral) SCC, using Time-constant (T) obtained with the velocity-step rotatory chair test for the overwhelming majority of the published data (Bischoff et al. 2005). It was estimated that the vestibular deterioration would start approximately 9 years earlier than the hearing decline, with a more rapid decline compared to the progression of hearing deterioration and with a complete loss of function of the horizontal SCC function already achieved in the 5th decade, which is well before the hearing decline has reached its endpoint (Bischoff et al. 2005).

The last decade was marked by the emergence of new diagnostic tools to clinically evaluate the vestibular system, such as the video head impulse test (vHIT) and vestibular-evoked myogenic evoked potentials (VEMPs). This expanded the vestibular evaluation to all six SCCs and the otolith organs (saccule and utricule) (Curthoys 2010; Curthoys et al. 2012; Halmagyi et al. 2017). Meanwhile, electronystagmography (ENG) was complemented by videonystagmography (VNG) in many vestibular laboratories. The former tools, however, were not available at the time of the earlier studies, which were mainly reporting on symptomatic carriers that already had established BVP.

The aim of this study was to comprehensively evaluate vestibular function in the largest series of 111 Belgian and Dutch p.P51S presymptomatic as well as symptomatic carriers using ENG/VNG, vHIT, and VEMPs. By doing this, we aimed: (1) to determine which part of the vestibular sensor showed the first signs of deterioration; (2) to study at what age SCCs and otolith function started to deteriorate; (3) to determine the age at which p.P51S variant carriers developed caloric areflexia on VNG and impaired vHIT VOR-gain as defined by the Barany Society criteria for BVP; and (4) to establish the chronology or sequence (hierarchy) by which different locations of the otovestibular end organ tend to deteriorate in p.P51S carriers.

MATERIALS AND METHODS

Ethics Approval

The study was designed and conducted according to the Declaration of Helsinki (1996) and it was approved by the local ethics committees of the Antwerp University Hospital of Antwerp and the Hasselt Jessa Hospital (B300201630243) (Dale & Salo 1996). The study was registered in ClinicalTrials.gov (NCT03716908, updated August 21, 2019).

Enrollment, Inclusion, and Exclusion Criteria

Patient identification, enrollment and otovestibular investigations started from January 1, 2019 and ended on January 31, 2020 and were carried out in the University Hospital of Antwerp and Jessa Hospital of Hasselt, Belgium.

All confirmed carriers of p.P51S variant of at least 18 years of age were eligible for enrollment. The following exclusion criteria were used: all siblings younger than 18 years at the time of investigation, conductive hearing loss (difference of at least 15 dB HL between air and bone conduction measured on at least three subsequent frequencies), sensorineural hearing loss due to other concomitant disease, vestibular dysfunction due to other causes than DFNA9, previous middle ear surgery, known neurological disorders, known cerebral/cerebellar disorders, intracranial disease/tumors, unwillingness or inability to undergo thorough audiological and vestibular examination, and contraindication for VNG and/or vHIT, such as ear drum perforation, chronic ear disease, cervical pathology, etc.

Age Groups

The subjects' age was allocated according to the age at the time of investigation. All subjects were separated into six groups (3rd decade, 18–29 years of age; 4th decade, 30–39 years; 5th decade,40–49 years; 6th decade, 50–59 years; 7th decade, 60–69 years; and 8th decade, 70–80 years.

Vestibular Testing

VNG was carried out in both centers, and it was performed in a sound-treated and semidarkened room with the patient's eyes open.

In the Hasselt center, VNG was administered using the DI 140500 NysStar I with the DiSoft II package (Difra, Welkenraedt, Belgium) with water irrigation as the caloric stimulus (Aquastar; Difra). The patients were wearing a NysStar I goggle (Difra) with a removable camera on one eye and the other eye shielded. In contrast, the Otometrics ICS Chartr 200 VNG (Natus, Taastrup, Denmark) was used in the Antwerp Center with air irrigation as the caloric stimulus.

Bilateral caloric irrigation was used to evaluate low-frequency lateral SCC function. The methodology and normative values were reported earlier by Van der Stappen et al. (2000) and Wuyts et al. (2007). To summarize, caloric tests were administered with the subject in supine position, with a head elevated 30° to align the horizontal (lateral) SCC vertically for maximal stimulation. Eye movements were calibrated before each caloric test and the subject was distracted using mental arithmetic. Bi-thermal caloric irrigations at 30°C (cold irrigation) and 44°C (warm irrigation) were performed in a 30-second time span (180 ml) for both stimulations, with a fixed stimulation sequence (cold left, cold right, warm left, and warm right). A minimum of 5-minute interval was kept between successive caloric irrigations, and it was prolonged in case the caloric nystagmus was still measurable after this time span until disappearance of the caloric induced nystagmus. For the caloric responses elicited with air as a stimulus, cold and warm irrigation were set at 25°C and 44°C, respectively, with a stimulation time of 60 seconds.

The eye-tracker trace was continuously monitored during the full length of the VNG examination. All artifacts were digitally erased by the examiner (first author) from the raw signals after each test sequence to avoid biased results. The bi-thermal 30°C to 44°C sum of maximal peak slow-phase velocity (SPV) (°/s) per ear was calculated for both labyrinths per subject, which were both used for analysis. Normative values from a matched control group were used in each vestibular laboratory.

vHIT was administered in a well-lit room by the same investigator for each center (the first author for the Hasselt center and the second author for the Antwerp center). The methodology and normative values were outlined elsewhere (Halmagyi et al. 2017). To summarize, the vHIT procedure was administered with the examiner standing behind the subject, who was sitting at 1.5 m in front of a fixed visual target at eye level. The goggles (Otometrics, Taastrup, Denmark) were equipped with a fixed infrared camera record recording the right eye. Head impulses were delivered in pairs according to the plains of each SCC until 10 valid head impulses were recorded for each direction, respecting the following sequence: left lateral/right lateral (LL/RL), left anterior right posterior, and right anterior left posterior. The main outcome parameter was vHIT VOR-gain (by evaluating the relation between eye and head velocity). According to the Barany criteria for bilateral vestibulopathy, the cutoff vHIT VOR-gain value of <0.6 was used to categorize vHIT gains as abnormal for each SCC (Strupp et al. 2017). We used VOR-gains, obtained by the device with artifact reduction, of all SCCs from both labyrinths for analysis.

The VEMPs using both C-VEMP (cervical: air-conducted saccular testing) and O-VEMP (ocular: air-conducted utricular testing) were administered, following the methodology outlined in previous studies (Maes et al. 2010; Curthoys et al. 2012; Vanspauwen et al. 2017). For C- (and O-) VEMP tests, the subject was placed in a supine position to allow higher muscle contraction (against gravity force). Constant muscle tensions and comparable left-right muscle tension throughout the whole recording were achieved with the self-monitoring system of the Neuro Audio AEP system (Difra, Welkenraedt, Belgium) under supervision of the investigator. An air conduction sound stimulus was used at 500 Hz, low-filter 30 Hz, high-filter 2000 Hz, range 1 mV, stimulation rate 5 Hz, maximal stimulus counts 150, analysis time window 50 ms, 50-Hz notch filter on, notch filter type alternative, acquisition 5 ms sweep, sensitivity 40 μV, averaging 5 ms sweep, sensitivity 40 μV (for both C- and O-VEMPs). The evoked C-VEMPs were recorded with surface electrodes placed at the midpoint of the ipsilateral Sternocleidomastoid Muscle (SCM), with the reference electrode on the upper part of the sternum and the ground (common) on the forehead. Impedances were checked and accepted if below 4 kΩ. Biphasic waveform with initial positive polarity (P1) and subsequent negative (N1) within 30 msec after stimulus were accepted as positive C-VEMP responses. Each run consisted of at least 60 averaged sweeps. For the C-VEMP, threshold measurements were administered using the Hood method (−10/+5 dB) ipsilaterally for both sides, starting from 110 dB nHL. In case, no responses were detected, an arbitrary value of 120 dB HL was allocated. The O-VEMPs were obtained with air conduction and were only carried out in the Hasselt center. Two active electrodes placed on the lower eyelids and two reference electrodes placed just underneath them, with a common (ground) electrode on the forehead. Each run consisted of at least 100 sweeps meanwhile contralateral recording was performed during up-gaze at a fixed point of the sealing (30° up-gaze from resting gaze). Biphasic waveform with initial n10

response within 12 msec was accepted as a positive signal. C- and O-VEMPs of both labyrinths were used for analysis.

The O-VEMPs were administered to 30 p.P51S carriers in the Hasselt center (27% of all participants). Since the bone conduction Mini-shaker was unavailable due to CE label issues, these were performed by air conduction.

Statistical Analysis

For statistical analysis and graphic illustrations, R software Version 1.3.1056 (R: a language and environment for statistical computing, Vienna, Austria) was used.

Comparisons between numeric and categorical data were analyzed using unpaired Welsh two sample t-test, ANCOVA or Mann–Whitney *U* tests depending on equality of variances. One sample t test was used to compare means with age-referenced limit. Statistical significance was fixed at $p < 0.05$, unless Bonferroni correction was justified.

Nonlinear "drc"-regression (CRAN "drc"-package in R) and simple linear regression were calculated for relationships between numeric variables depending in linearity of the relationship between the variables.

The following parameters were used for statistical analysis: age (years), hearing deterioration ($PTA^{0.5–4}$ [0.5–4 kHz], $PTA^{4–8}$ [4–8 kHz] and $PTA^{6–8}$ [6–8 kHz], dB HL) bi-thermal 30°C to 44°C (or 25°C–44°C for air stimulation) sum of maximal peak SPV (°/s), vHIT VOR-gains obtained from lateral (horizontal, LSCC), anterior (superior, SSCC), and posterior (PSCC) SCC as well as the averaged gain of all three SCCs per side, C-VEMP both numerical (threshold, dB nHL) and categorical (present or absent) and O-VEMP response as categorical (present or absent).

The presence or absence of the O-VEMP response was compared with the following parameters: age (years), $PTA^{0.5–4}$ (0.5–4 kHz) dBHL, $PTA^{4–8}$ (4–8 kHz), and $PTA^{6–8}$ (6–8 kHz) (dB HL), caloric bi-thermal maximal peak SPV (°/s), vHIT VOR-gains of lateral (horizontal) (LSCC), anterior (SSCC) and PSCC separately (plus the average gain of the three SCCs per labyrinth) and the C-VEMP thresholds (dB nHL), applying Mann–Whitney *U* tests to test for significant difference in medians in the case of the presence of O-VEMPs compared to the absent O-VEMP signal. The same was applied for the C-VEMPs as categorical (present or absent signal).

In the following sections, the methodology for the determination of normative value, age of onset and decline rate (slope) of the different vestibular end-organs is further developed in detail.

Determining Normative Values

Before determining the age of onset of the vestibular function in its different sensory parts (low-frequency caloric response, high-velocity SCC response on head impulse and otolith function [vestibular myogenic evoked response]), normative values for all vestibular tests had to established first, before comparing these with data of the study population.

For this purpose, p50th and p95th percentile normative values were derived from a matched control group for each vestibular end-organ function (caloric SPV [VNG], vHIT VOR-gain and C-VEMP threshold). The statistical distribution of caloric bi-thermal maximal peak SPV (°/s), vHIT VOR-gain and C-VEMP threshold (dB nHL) in relation to age were achieved by calculating the median (p50th) and the distribution around the median using upper or lower halves of Gaussian distribution and corresponding standard deviation (median + [standard deviations × 2]) ($p95^{th}$). The caloric bi-thermal maximal peak SPV (°/s), vHIT VOR-gain or C-VEMP threshold deviation, which can be expected to be exceeded by 50% (median) and 95% of a vestibular normal population of a given age, were obtained for the p50th and p95th percentile values of the three vestibular tests, respectively.

Water Versus Air Stimulation in Caloric Test

As described in the section "Determining Normative Values," different testing paradigms were used during VNG by the two centers for the caloric tests, namely water irrigation by the Hasselt group and air irrigation in Antwerp.

For this reason, the bi-thermal sum of maximal peak SPV of water (30°C–44°C; duration of 30 seconds) and air (25°C–44°; duration 60 seconds) irrigation were collected separately. Since ANCOVA analysis to compare means of caloric SPV in relation to age with both test paradigms (air versus water irrigation) was significantly different, the regression analysis of pooled water and air caloric responses was abandoned and analysis of caloric SPV obtained with water and air irrigation as a stimulus were conducted separately.

Determination of Age of Onset

Age of onset of vestibular deterioration for all different end-organs was estimated by applying both descriptive and inferential statistics in line with previous publications (Verstreken et al. 2001; Bom et al. 2003; Lemaire et al. 2003; Bischoff et al. 2005). For the former, which is a categorical approach, we used age as categorical variable (age pooled in decades ranging from 3rd to 8th) resulting in estimation of the age *decade* in which the vestibular function of each end-organ starts to deviate from age-referenced limits. Onset was determined by visual comparison of median with age-referenced limits and one-sample t test. For the inferential analysis, the estimation of age of onset was obtained using regression models and outcome was expressed in *years* (numeric approach).

Age of Onset in Decades

Box and Whisker plots with additional p50th and p95th percentile values were constructed for the following parameters: Caloric SPV (water irrigation [VNG water]) with age pooled in decades, caloric SPV (air irrigation [VNG air]) with age pooled in decades, caloric SPV (VNG water) with age pooled in 5-year intervals, caloric SPV (VNG air) with age pooled in 5-year intervals, vHIT VOR-gains of LSCC, SSCC, PSCC, the three SCC averaged (3SCC), and C-VEMP threshold. The start of the vestibular decline was definitely validated if the following criteria were met: (1) when the median of a given measured vestibular end-organ parameter of a given age group (decade or 5-year interval), would sustainably exceed the corresponding p95th percentile value at a particular decade; (2) when this was consistently observed across the following decades (or 5-year intervals); and finally (3) when validated using the one-sample t test for each vestibular end-organ function (as enumerated above), for each decade (or 5-year interval), separately. With a $p < 0.001$ as significance level, the observed mean of the sample was compared with the corresponding p95th percentile value (mμ) to test the null hypothesis (the observed mean of the sample is greater

or less than mμ), depending on the dependent variable. This was chronologically applied from the 3rd to 8th decade.

Caloric bi-thermal maximal peak SPV and vHIT VOR-gain cutoff values of, respectively, 6°/s and 0.6 were used according to the Barany criteria for vestibulopathy (Strupp et al. 2017). Normative values for C-VEMP thresholds, VNG caloric function, and vHIT test were determined from a matched control population which partly consisted of confirmed noncarrier siblings of p.P51S variant carriers.

Age of Onset in Years and Decline Rate (Slope)

To estimate age of onset as well as the progression of the vestibular dysfunction, regression was fitted on vestibular data (caloric bi-thermal SPV [°/s], VOR-gain of eye versus head movement during vHIT and C-VEMP-threshold [dB nHL]). In the case of nonnormality, box-cox transformations were applied to determine the most appropriate power transformation of the raw variables (here: log-transformation of caloric SPV). Because maximal C-VEMP thresholds (120 dBnHL) were believed to be reached quickly, there was a risk of a very limited range of data output, with a large fraction of values encoded as 120 dB nHL, which could bias regression analysis. In that case, a censored regression model fit would then be applied to deal with this problem, where all data output encoded with 120 dB nHL, or with absent response, would be fixed at 120 dB and regression would be applied to all values. This is fundamentally a different approach from truncated regression, where all data beyond a fixed point would have been removed.

In the case of S-shaped nonlinear relationship between dependent and independent variables, the nonlinear dose-response regression models (drc) were used, as applied in part I (auditory phenotypic expression of the p.P51S *COCH* variant).

Estimation of the age of onset and slope of vestibular dysfunction across the decades was carried out using linear regression of transformed data (VNG: caloric bi-thermal maximal peak SPV [°/s] for water and air irrigation separately), censored regression of C-VEMPs and nonlinear drc-regression (dose-response curve) of vHIT VOR-gains, with age as an independent variable. Separate models were fit for each of these variables. To compute the slope of vHIT VOR-gain decrease over ages (as a measure of annual vestibular deterioration [AVD]), the model function of the generalized log-logistic equation was used to calculate y1 (lower), y2 (upper) and estimate corresponding x1 (lower) and x2 (upper) values (estimates of effective dose or "ED"), as coordinates of the linear segment of the resulting (negative) S-shaped dose-response curve.

These coordinates were used to compute a simple regression model of the linear segment, with the slope or AVD and corresponding 95% confidence intervals as a result. The linear segment was delineated between 20% and 80% of progression.

Relationship Between VEMPs and Age, Auditory, and Vestibular Function in p.P51S Carriers

For the relationship between the presence of O-VEMP response and other variables (PTAs, caloric bi-thermal maximal peak SPV, vHIT VOR-gain, C-VEMP threshold), Mann–Whitney *U* test with Bonferroni adjustment ($p < 0.005$) was preferred instead of the independent two-sample t test in case the assumption of equal variances between both groups of the variable (present and absent O-VEMP response) would not be met in at least one variable. The same method was applied to study the relationship with the presence of absence of C-VEMP response.

Age-Related Typical Vestibulograms and Age-Related Typical Video HITs

"Age-related typical vestibulograms" (ARTV) and "age-related typical video HITs" (ARTvH) were built two ways: (1) with predictions derived from respective regression models for C-VEMPs, vHIT VOR-gains and VNG caloric gains, as previously outlined and (2) with means and 95% confidence intervals from the measured vHIT VOR-gain data as "observed" ARTV.

The ARTvHs were limited to the three SCC (LSCC, SSCC, and PSCC), whereas in the ARTV, caloric SPV and C-VEMP thresholds were added. This was applied for each decade (from 3rd to 8th decade) with the rescaling of the following vestibular parameters: C-VEMP threshold (dBnHL) (reversed values: i.e., [maximal output (120 dB nHL) – variable value]/30), VNG caloric bi-thermal maximal peak SPV with water irrigation as a stimulus (log(value)/3). The "predicted" vHIT VOR-gains of the three SCCs were derived from predictions using "drc"-regression model fit.

Deterioration Sequence (Hierarchy) of Auditory and Vestibular Function in p.P51S Carriers

To determine and visualize a possible p.P51S mutation-specific decline hierarchy or sequence of all different cochleovestibular end organs, estimated ages of onset of dysfunction were summarized and plotted according to ascending chronology at time of presentation, both according to estimates derived from regression analysis (age in years) as well as to visually endorsed onset age in decades.

RESULTS

Age and Gender Distribution of Study Population

From January 1, 2019 till January 30, 2020, 111 confirmed p.P51S *COCH* variant carriers (222 labyrinths) were enrolled for the study and underwent all investigations as outlined in the methodology section. Despite aging demographic distribution in most of the studied family pedigrees, 22 asymptomatic carriers aged under 40 years were included. The male/female ratio was 55/56. There were no statistically significant differences in hearing thresholds between both genders at any frequency nor hearing index (Welsh two sample t-test). Similarly, there were no significant differences in caloric bi-thermal maximal peak SPV, vHIT VOR-gain, and C-VEMP thresholds between both genders (see Table in Supplemental Digital Content 1, http://links.lww.com/EANDH/A821). Therefore, all male and female statistics were treated as one. The demographics of the study population was summarized in Table 1 and age distribution was depicted in Figure in Supplemental Digital Content 1, http://links.lww.com/EANDH/A821). The means and variances of vHIT VOR-gains were not significantly different between both centers (Hasselt and Antwerp; Welsh two sample t test, significance level $p < 0.01$, Supplemental Digital Content 1, http://links.lww.com/EANDH/A821).

TABLE 1. Demographics of study population, all carriers of the p.Pro51Ser COCH mutation (P51S) (n = 111)

Age (Decade)	Age (Mean)	Age (Range), yrs	Number (Ears)	Number Male (Ears)	Number Female (Ears)	Standard Deviation
3rd	22.4	(18–25)	10	2	8	2.55
4th	35.19	(30–39)	32	18	14	3.10
5th	45.44	(40–49)	42	26	16	2.61
6th	54.96	(50–59)	52	16	36	2.70
7th	64.54	(60–69)	58	34	24	2.12
8th	75.07	(70–80)	28	12	16	3.18

Caloric Response Versus Age

In none of the subjects, the caloric tests had to be interrupted prematurely. As expected, there was a considerable difference in amplitude of caloric responses expressed in maximal peak SPV amplitudes (°/s) between those obtained with water versus air irrigation (caloric stimulus), as depicted in Figure 1. There were three- to four-fold higher values of maximal peak SPV with water stimulus. Moreover, the decline rate (decrease of SPV per year) of water-induced caloric response was different from that of air stimulation. Bi-thermal sum of maximal peak SPV of both stimulus groups were significantly different ($p < 0.001$, ANCOVA analysis, with age as an independent and VNG test paradigm (air versus water) as a dependent variable).

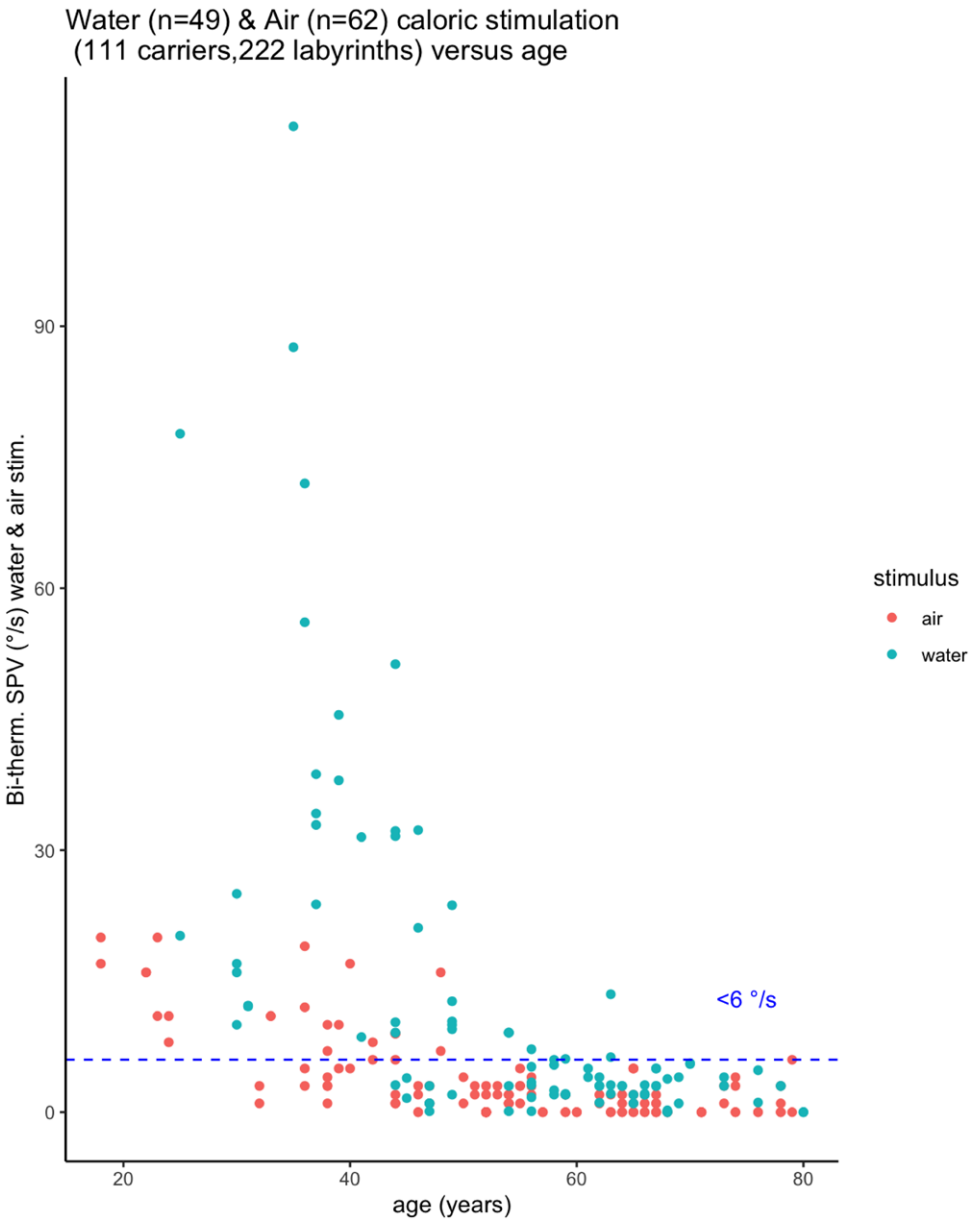

Fig. 1. Age-related bi-thermal maximal peak SPV (°/s) of caloric responses elicited with both water (red dots) and air (blue dots) stimulation. Note the considerable difference in amplitude and scale of the responses between water and air stimulation. The Barany Society BVP cutoff value of 6°/s is reached much earlier for the air stimulus. BVP, bilateral vestibulopathy; SPV, slow-phase velocity.

For those reasons, the determination of the age of onset was achieved for caloric gain obtained with both air and water irrigation separately. Box and Whisker plots were plotted against age with superimposition of normative p95th percentile values, obtained from matched control group in respective vestibular laboratories, as outlined in the section "Age and Gender Distribution of Study Population" (Fig. 2).

Maximal peak SPV values under 6°/s, obtained with bi-thermal 25°C tot 44°C air stimulation (duration: 60 seconds), were reached earlier compared to water stimulus, as shown in Figure 2. When applying the lower p95th normative values of each vestibular laboratories (water and air stimulus separately), the average age of onset of caloric response decline and of areflexia (BVP) were both reached in the 4th decade for the air stimulus group, whereas hyporeflexia and BVP were observed in the 5th and 6th decades, respectively, for the water stimulus group. To better define the age of onset of caloric decline, age was also plotted in increments of 5-year interval against SPV values to

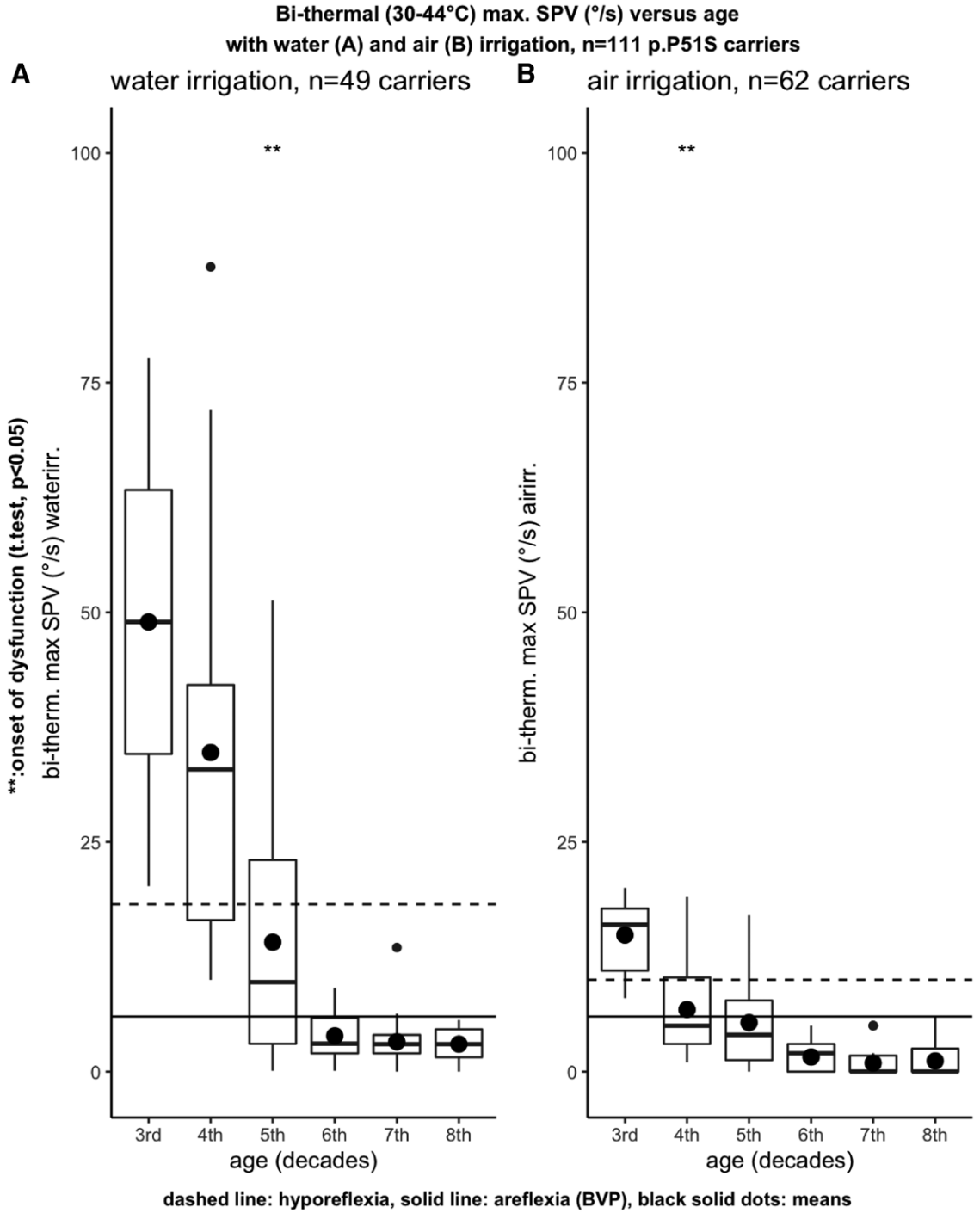

Fig. 2. Dashed line: limit line for hyporeflexia, solid line: limit line for BVP (6°/s) as defined by the Barany Society. Caloric bi-thermal 30°C–44°C maximal peak SPV bi-thermal SPV versus age using water (A) and air (B) stimulus. Note the different ages of onset between caloric responses with air versus water irrigation. SPV, slow-phase velocity.

illustrate the progression more in detail (Fig. 3). Median SPV values, obtained using the water stimulation paradigm, exceeded the lower p95th percentile for hyporeflexia in the age interval of 45 to 49 years compared to 30 to 34 years for air stimulation. Maximal peak SPV values under 6°/s, obtained with bi-thermal 30°C to 44°C water irrigation, were observed at an age between 50 and 54 years in contrast with air stimulation (40–44 years) (Fig. 3). Estimations of the age of onset and areflexia (maximal loss) of the caloric gain as well as the AVD (or slope) with both water and air irrigation paradigm are summarized in Table 2.

vHIT Versus Age

Age-related vHIT VOR-gain deterioration is represented for each SCC in Figures 4 and 5 and summarized in Table 2. The onset of VOR-gain decrease of the PSCC was observed at an average age of 48 years (5th decade), whereas this was estimated at 52 years on average and 57 years for the LSCC and SSCC, respectively (6th decade) (Figure 5). The vHIT VOR-gain of the posterior SCC reached maximal loss at an average age of 79 years. The vHIT VOR-gain of less than 0.1 was estimated at an average age of 85 years at the level of the SSCC and LSCC (Table 2).

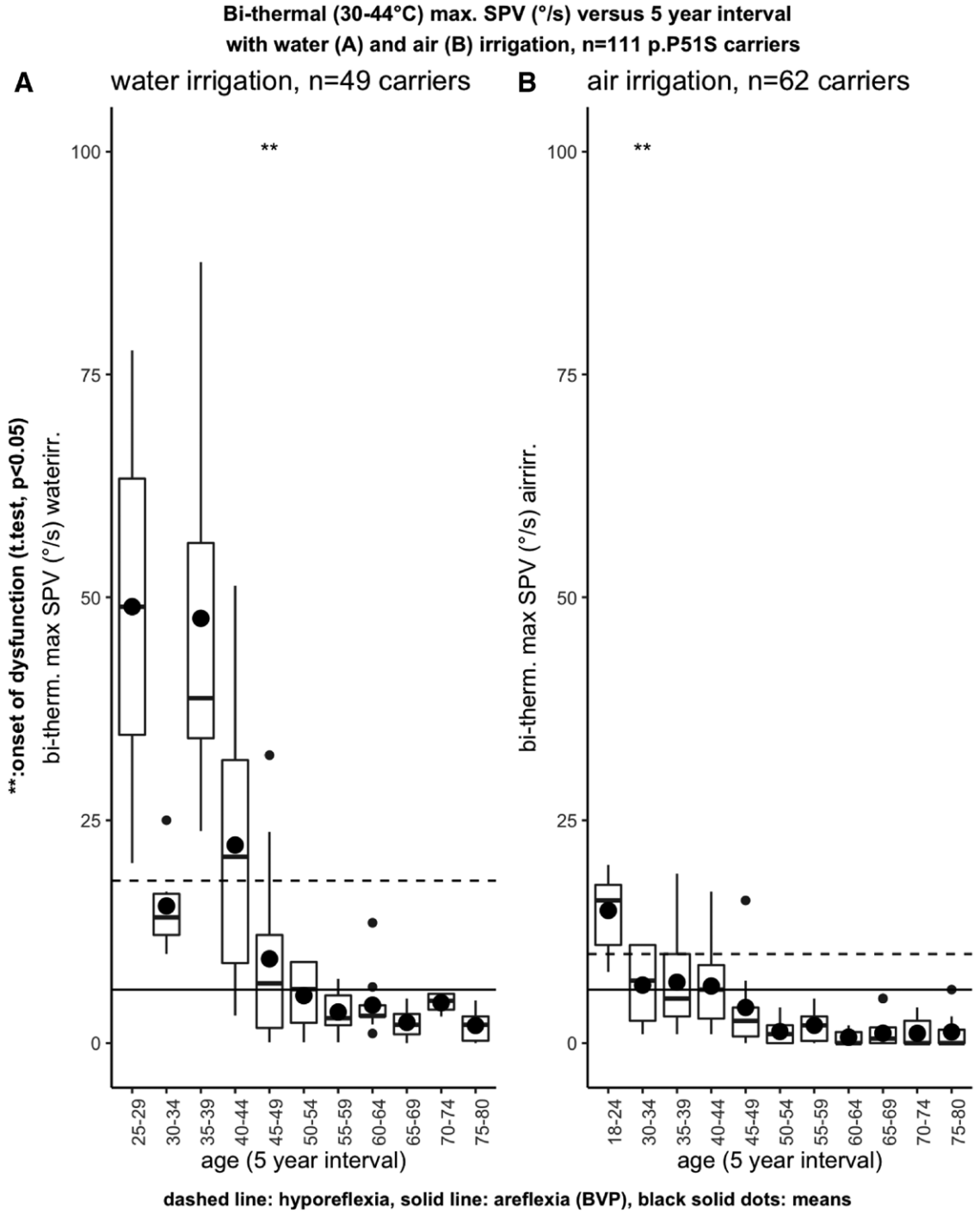

Fig. 3. Dashed line: limit line for hyporeflexia, solid line: limit line for BVP (6°/s) as defined by the Barany Society.Caloric response obtained with bi-thermal 30°C–44°C sum of maximal peak SPV with water and air stimulus in 111 p.P51S variant carriers, 5-year interval. SPV, slow-phase velocity.

TABLE 2. Estimates of average milestone ages of vestibular deterioration in p.P51S COCH variant carriers (average age of onset and age of maximal loss), (A) caloric maximal peak SPV, (B) vHIT VOR-gain, and (C) C-VEMP threshold

A VNG Caloric Test	Slope (Annual Vestibular Deterioration) (°/s/yrs)	Age at Start Decline (yrs)	Age at Areflexia (<6°/s)
Water irrigation (n = 49)	–5.067 (95% CI, –5.762; –4.371)	35.397 (95% CI, 20.218; 62.086)	52.813 (95% CI, 34.468; 84.432)
Air irrigation (n = 62)	–3.293 (95% CI, –3.760; –2.826)	25.085 (95% CI, 12.582; 45.957)	31.069 (95% CI, 17.600; 53.362)
B	Slope (annual vHIT VOR-gain deterioration) (gain/yrs)	Age at start gain (<0.6) BVP	Age at maximal gain loss (<0.1)
vHIT averaged VOR-gain of 3 SCC/labyrinth	–0.019 (95% CI, –0.023; –0.014)	51.176 (95% CI, 36.210; 66.143)	87.045 (95% CI, 69.300; 99.065)
vHIT LSCC VOR-gain	–0.018 (95% CI, –0.024; –0.012)	51.785 (95% CI, 29.063; 74.509)	85.045 (95% CI, 75.059; 104.860)
vHIT SSCC VOR-gain	–0.021 (95% CI, –0.017; –0.010)	56.649 (95% CI, 43.629; 69.832)	84.668 (95% CI, 69.019; 106.116)
vHIT PSCC VOR-gain	–0.014 (95% CI, –0.017; –0.010)	47.505 (95% CI, 43.066; 51.943)	78.595 (95% CI, 64.778; 99.669)
C	Slope (annual C-VEMP deterioration) (dB/yrs)	Age at start decline (yrs)	Age at maximal signal loss (yrs)
C-VEMP threshold (dB nHL) (n = 74)	1.067 (95% CI: 0.760; 1.369)	31.386 (95% CI: 13.029; 64.466)	45.485 (95% CI: 23.976; 84.210)

CI, confidence interval; LSCC, lateral semicircular canal; PSCC, posterior semicircular canal; SPV, slow-phase velocity; SSCC, superior semicircular canal; VEMP, vestibular-evoked myogenic evoked potentials; vHIT, the video Head Impulse Test; VOR, vestibulo-ocular reflex; VNG, videonystagmography.

vHIT Versus VNG

Four merged graphs of caloric maximal peak SPV responses (°/s), elicited with both water and air stimulus in a total of 222 labyrinths (111 p.P51S variant carriers), were summarized in Figure 6. A considerable number of labyrinths showed normal laterals SCC (LSCC) vHIT VOR-gain (>0.8) meanwhile presenting maximal peak SPV values that were already measured lower than cutoff p95th percentile values (i.e., water stimulus: 18.22°/s, air stimulus: 10°/s), which was also observed when caloric SPV decreased below Barany criteria for BVP (i.e., <6°/s). This number was considerably higher with water than air stimulus. Very few p.P51S variant carriers showed both normal caloric and vHIT VOR responses when air was used for stimulation in VNG tests compared to those obtained with water irrigation.

Age-Related C-VEMP Thresholds

As outlined in the previous section, censored regression was applied to compute slope and to estimate the age of onset and maximal deterioration of C-VEMP threshold, with a tobit fixed at 120 dB nHL (Table 2). Similar with the other variables (caloric response and vHIT VOR-gains), normative values of C-VEMP thresholds from 42 matched controls were determined and superimposed as p95th and p50th percentile values on Box & Whisker plots as illustrated in Figure 7. Mann–Whitney *U* tests were applied to test the relationship between the presence or absence of C-VEMPs and aging (decades). Increasing age of the p.P51S carriers was associated with absence of C-VEMP response, which was significant ($p < 0.01$) in all decades, except for the 3rd decade ($p = 0.483$ [3rd decade]). In the 5th decade, there was a rapid increase of the thresholds, whereas in most of the recordings in the 6th decade, response was not detectable. It is noticeable that values had high variability across all ages compared to the control group.

C-VEMP and O-VEMP Versus Age, Auditory, and Vestibular Function in p.P51S Carriers

For all parameters, there was a highly significant relationship between the presence of O-VEMP response with younger age, lower PTAs, higher caloric SPV (water irrigation), higher vHIT VOR-gains of all 3 SCCs and lower C-VEMP thresholds.

More specifically, in the case of positive O-VEMP response, p.P51S carriers where on average 20 years younger (39 versus 59 years) had a hearing advantage of at least 60 dB HL on average (10 versus 70 dB HL), showed caloric SPV that were five times as higher (28.25°/s versus 3°/s), vHIT VOR-gain values at least double as important (0.95 versus 0.47), and C-VEMP thresholds 30 dB nHL lower (90 versus 120 dB nHL) compared to carriers without O-VEMP responses.

Tables 3 and 4 summarize the relationship between the presence of a VEMP response with hearing and vestibular function, as well as age, for O-VEMPs and C-VEMPs respectively, using the Mann–Whitney *U* test. For both VEMPs, the presence of a response was significantly associated with younger age, better hearing levels, higher caloric SPV, and better vHIT VOR-gains at any SCC.

As explained in the Materials and Methods section, validation of the age of onset (in decade) of respective vestibular end-organ dysfunction was achieved using one-sample t test, which was summarized in Table 5. By applying this chronologically from 3rd to 8th decade, one can observe increasing C-VEMP thresholds and the absence of response already in the 3rd decade, followed by decrease of caloric SPV (water irrigation) and vHIT VOR-gain of the PSCC in the 5th decade, whereas the LSCC and SSCC were the last to show decreasing gains (6th decade).

ARTV, ARTvH, and Decline Hierarchy

Similar to the "age-related typical audiograms" (ARTA), as they were constructed with auditory data in part I, the deterioration of vestibular end organs in relation to aging was plotted for each decade to display a clear overview of the progression of the vestibular decline across the decades.

These "ARTV" and "ARTvH" were built with predictions derived from respective regression models for C-VEMPs, vHIT VOR-gains, and VNG caloric gains, as previously outlined and represented in Figure 8 ("predicted" ARTV and ARTvH) as well as with observed data ("observed" ARTV and ARTvH [Figs. 9 and 10]). Figure 4 in Supplemental Digital Content 1, http://links.lww.com/EANDH/A821, represent ARTV and ARTvH, including corresponding 95% confidence intervals.

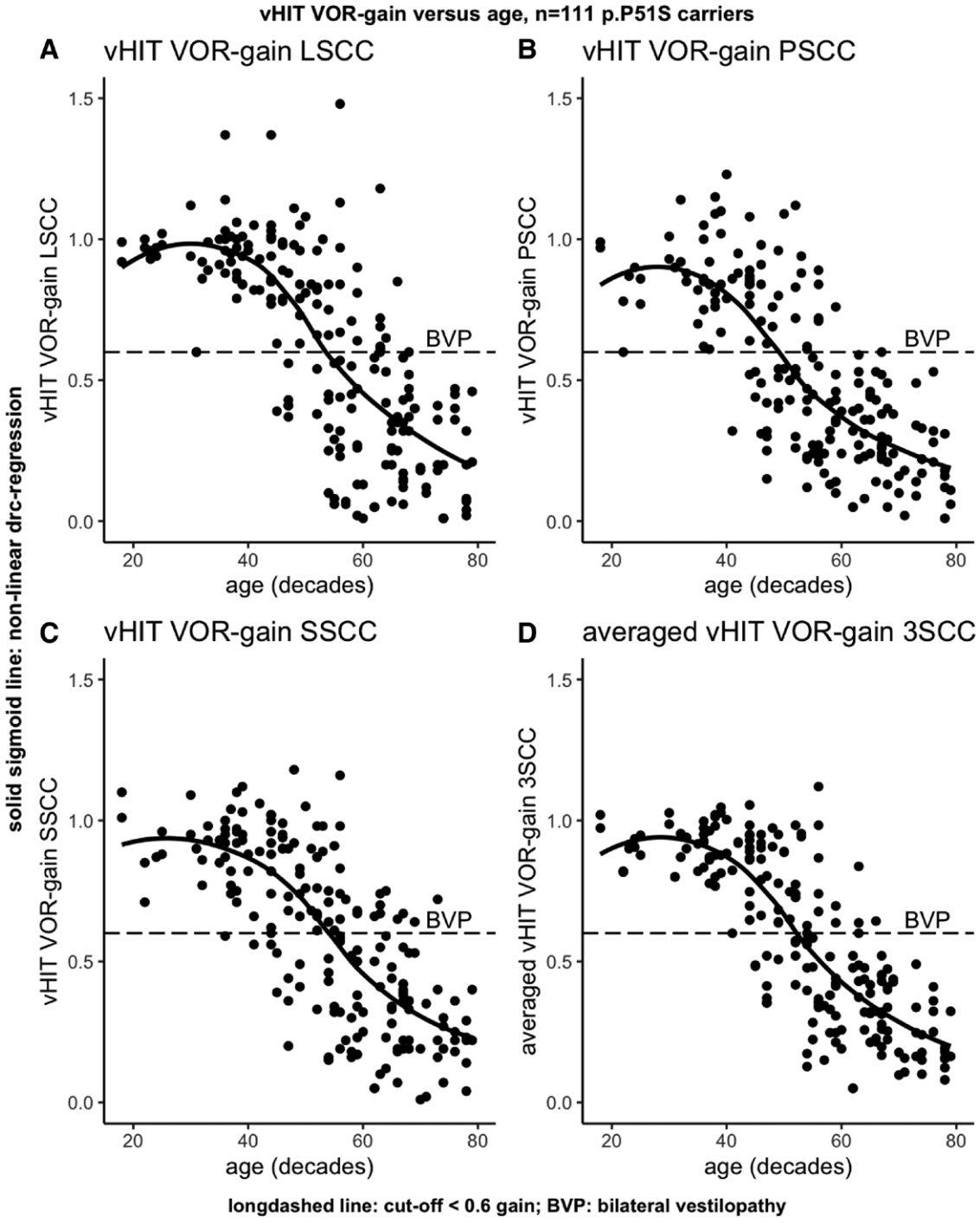

Fig. 4. vHIT VOR-gains versus age (n = 111 p.P51S carriers, (A) average vHIT VOR-gains of lateral SCC, (B) vHIT VOR-gains of Posterior SCC, (C) vHIT VOR-gains of Superior SCC, and (D) vHIT VOR-gains of all three SCC/labyrinth. BVP, bilateral vestibulopathy; SCC, semicircular canal; vHIT, the video Head Impulse Test; VOR, vestibulo-ocular reflex.

Tables 5–7 and Figure 11A and B summarize the sequential onset of dysfunction for each end organ in p.P51S carriers. Distinction was made between male and female audiological data, whereas caloric bi-thermal maximal peak SPV obtained with water and air irrigation were reported separately. Figure 11A shows high-frequency loss (6 and 8 kHz) presenting at first (in female carriers only), whereas the onset of the decline of the lower hearing frequencies (and all hearing frequencies in male carriers) was preceded by both C-VEMP threshold shift as well as decrease of bi-thermal maximal peak SPV values on VNG elicited with water irrigation by 9 years. The vHIT VOR-gains are the last end-organ location to show decline offset. The auditory deterioration shows an acceleration between 40 and 50 years (5th–6th decade).

In contrast, when the age of onset of deterioration was determined using the categorical way (Fig. 11B), caloric bi-thermal maximal peak SPV deterioration starts simultaneously with

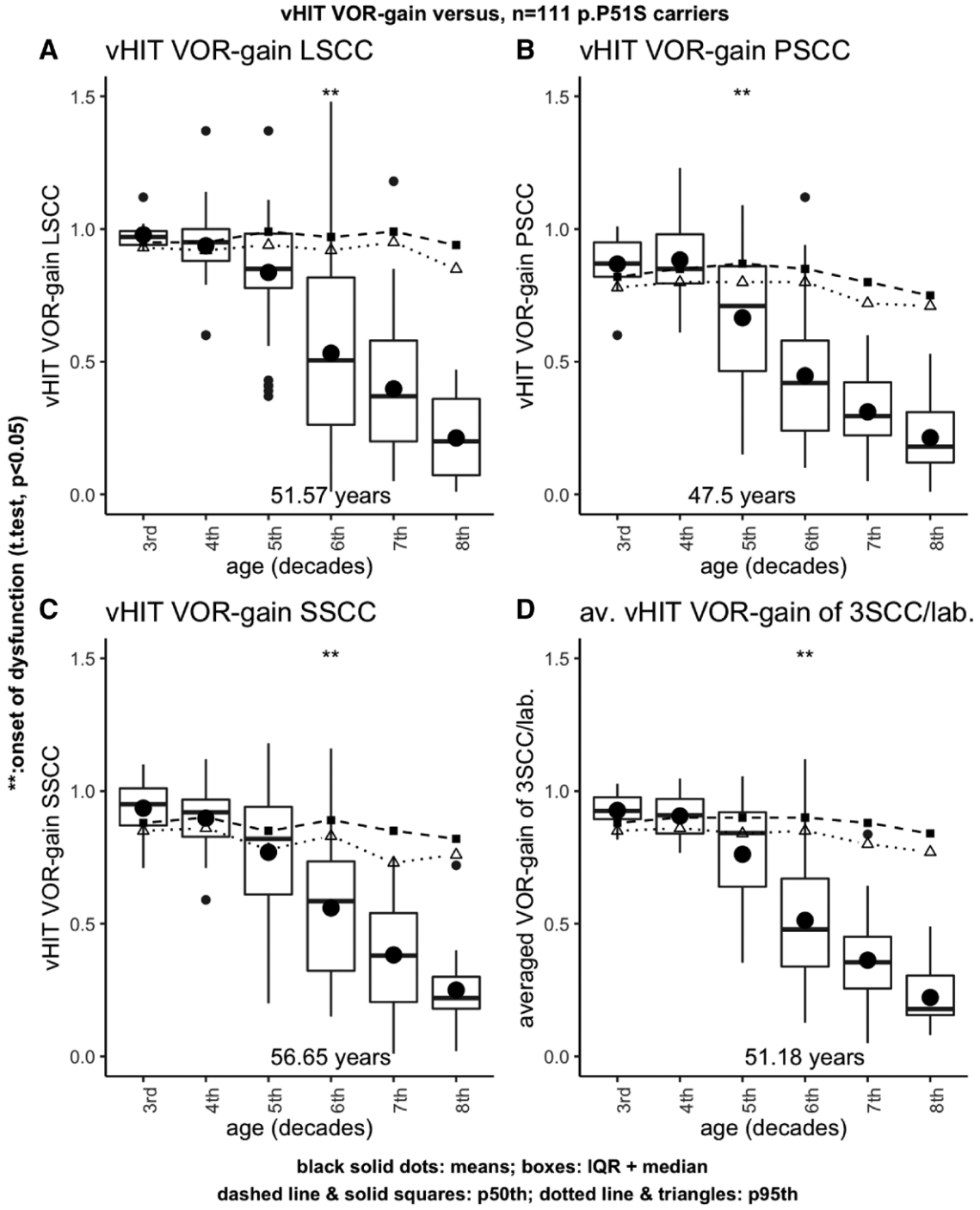

Fig. 5. vHIT VOR-gains derived from all three SCCs per labyrinth separately and averaged VOR-gains of all three SCC per labyrinth (n = 111 p.P51S carriers). Note that the "starting point" (vHIT VOR-gain < 0.6) are observed in the 6th decade for all SCC, except for the PSCC (5th decade). The dashed lines with solid squares represent the p50th percentile values obtained from a matched control group, and the dotted lines with open triangles are the p95th percentile. PSCC, posterior semicircular canal; SCC, semicircular canal; vHIT, the video Head Impulse Test; VOR, vestibulo-ocular reflex.

PSCC vHIT VOR-gains and with hearing function in male carriers and the majority of hearing frequencies in female carriers. C-VEMPs and hearing function at 6 and 8 kHz in female carriers all begin their decline in the 3rd decade, whereas vHIT VOR-gains at the LSCC and SSCC are the last to deteriorate (Tables 6 and 7).

DISCUSSION

The main scope of the present study was to investigate the vestibular function of the largest series of p.P51S variant carriers (n = 111), including presymptomatic carriers and using a vestibular test battery which enables a better coverage of the frequency range of the vestibular sensorineural function. For this purpose,

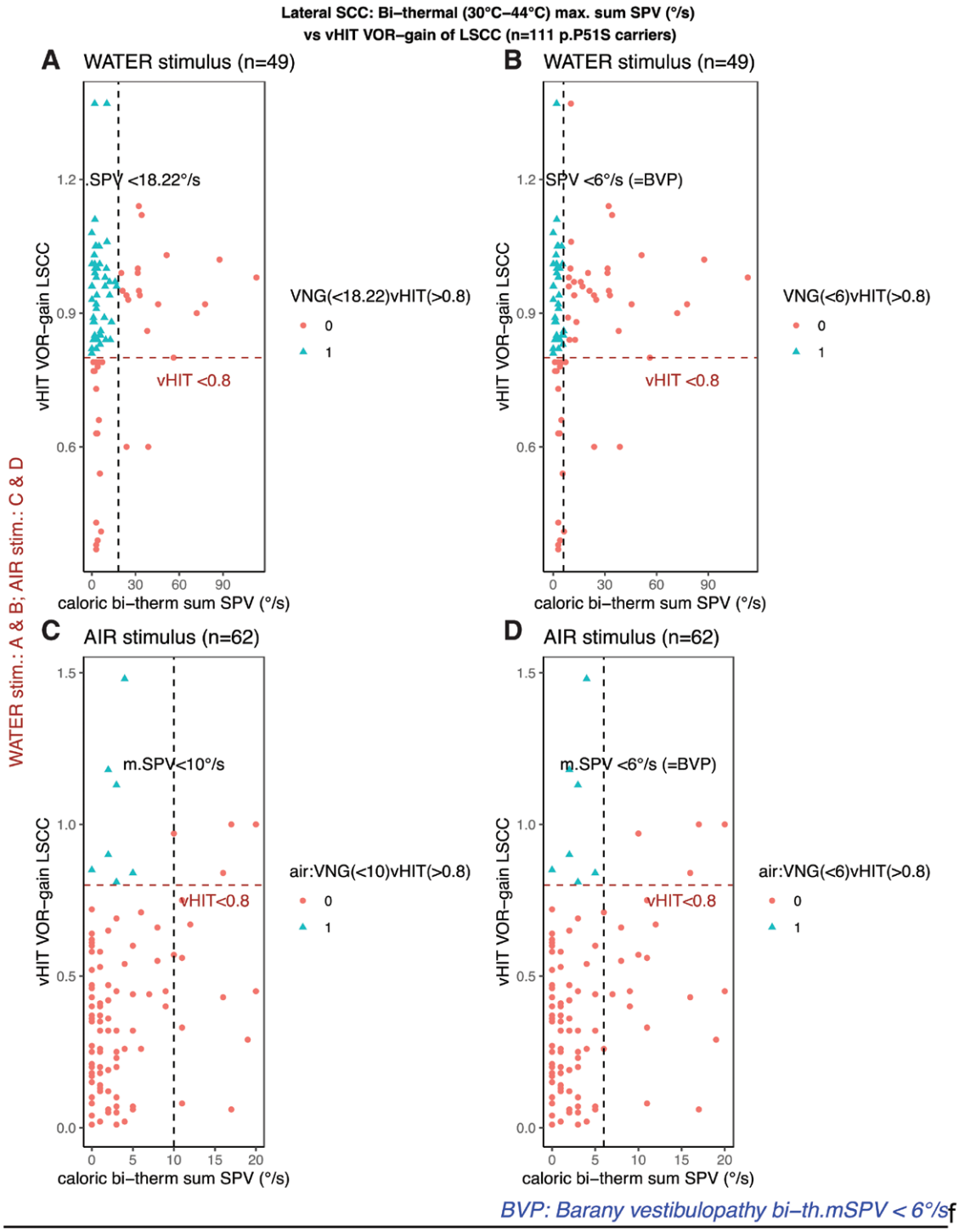

Fig. 6. vHIT VOR-gains of the LSCC versus caloric bi-thermal (30°C–44°C) sum of maximal peak SPV (°/s) in n = 111 p.P51S variant carriers. A and B, VNG caloric stimulus = water irrigation. C and D, VNG caloric stimulus = air irrigation. LSCC, lateral semicircular canal; SPV, slow-phase velocity; VNG, videonystagmography.

besides VNG caloric test, C- & O-VEMPs, and vHIT tests were administered as well.

The vestibular deterioration sequence was different between numeric (estimations based on log-transformed linear regression of VNG caloric data [with water and air irrigation separately] as well as censored regression of C-VEMP thresholds) and categorical approach (visual determination of offset age [endorsed with one sample t test]) in Figures 2, 3, and 8 (Table 2). Whereas VNG caloric gains visually started to decrease beyond age-referenced limits in the 5th decade with water irrigation, 4th decade with air irrigation and 3rd decade for C-VEMPs, the onset ages were, respectively, estimated about 36, 26, and 31 years on average. This apparent discrepancy may be explained by the wide confidence intervals of these estimations and the relativity with

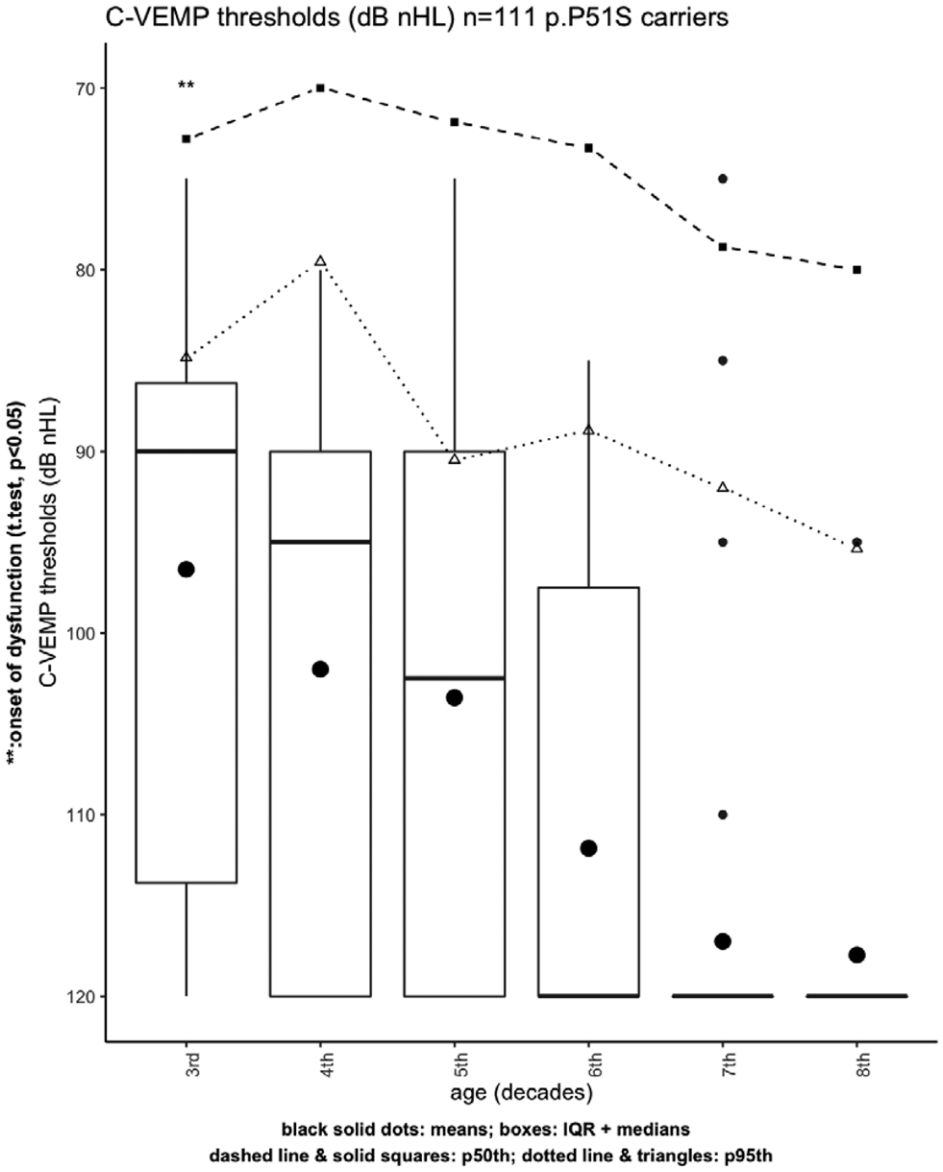

Fig. 7. C-VEMP Thresholds (dB nHL) versus age, n = 73 p.P51S carriers with normative values per age (decade). VEMP, vestibular-evoked myogenic evoked potentials.

TABLE 3. Relationship between the presence of C-VEMP signal with better hearing and vestibular function (Mann–Whitney U test with Bonferroni adjustment ($p < 0.001$)

	p	95% CI
Age	<0.001	11.000; 19.000
PTA 0.5–4 kHz	<0.001	35.000; 56.250
PTA 4–8 kHz	<0.001	22.500; 47.500
PTA 6–8 kHz	<0.001	23.000; 48.000
VNG water irr	<0.001	−27.600; −8.300
VNG air irr	<0.001	0.990; 2.000
vHIT 3 SCC	<0.001	−0.320; −0.090
vHIT LSCC	<0.001	−0.370; −0.120
vHIT SSCC	<0.001	−0.290; −0.100
vHIT PSCC	<0.001	−0.310; −0.080

CI, confidence interval; LSCC, lateral semicircular canal; PSCC, posterior semicircular canal; PTA, pure-tone average; SSCC, superior semicircular canal; VEMP, vestibular-evoked myogenic evoked potentials; vHIT, the video Head Impulse Test; VOR, vestibulo-ocular reflex; VNG, videonystagmography.

TABLE 4. Relationship between the presence of O-VEMP signal with better hearing and vestibular function (Mann–Whitney U test with Bonferroni adjustment ($p < 0.001$)

	p	95% CI
Age	<0.001	18.000; 27.000
PTA 0.5–4 kHz	<0.001	50.000; 67.500
PTA 4–8 kHz	<0.001	47.500; 77.500
PTA 6–8 kHz	<0.001	47.500; 72.500
VNG water irr	<0.001	−29.500; −13.000
VNG air irr*	NA	NA
vHIT 3 SCC	<0.001	−0.520; −0.350
vHIT LSCC	<0.001	−0.510; −0.290
vHIT SSCC	<0.001	−0.550; −0.300
vHIT PSCC	<0.001	−0.540; −0.330
C-VEMP	<0.001	20.000; 39.000

*No O-VEMP test was administered to those patients undergoing VNG with air irrigation.
CI, confidence interval; LSCC, lateral semicircular canal; PSCC, posterior semicircular canal; PTA, pure-tone average; SSCC, superior semicircular canal; VEMP, vestibular-evoked myogenic evoked potentials; vHIT, the video Head Impulse Test; VOR, vestibulo-ocular reflex; VNG, videonystagmography.

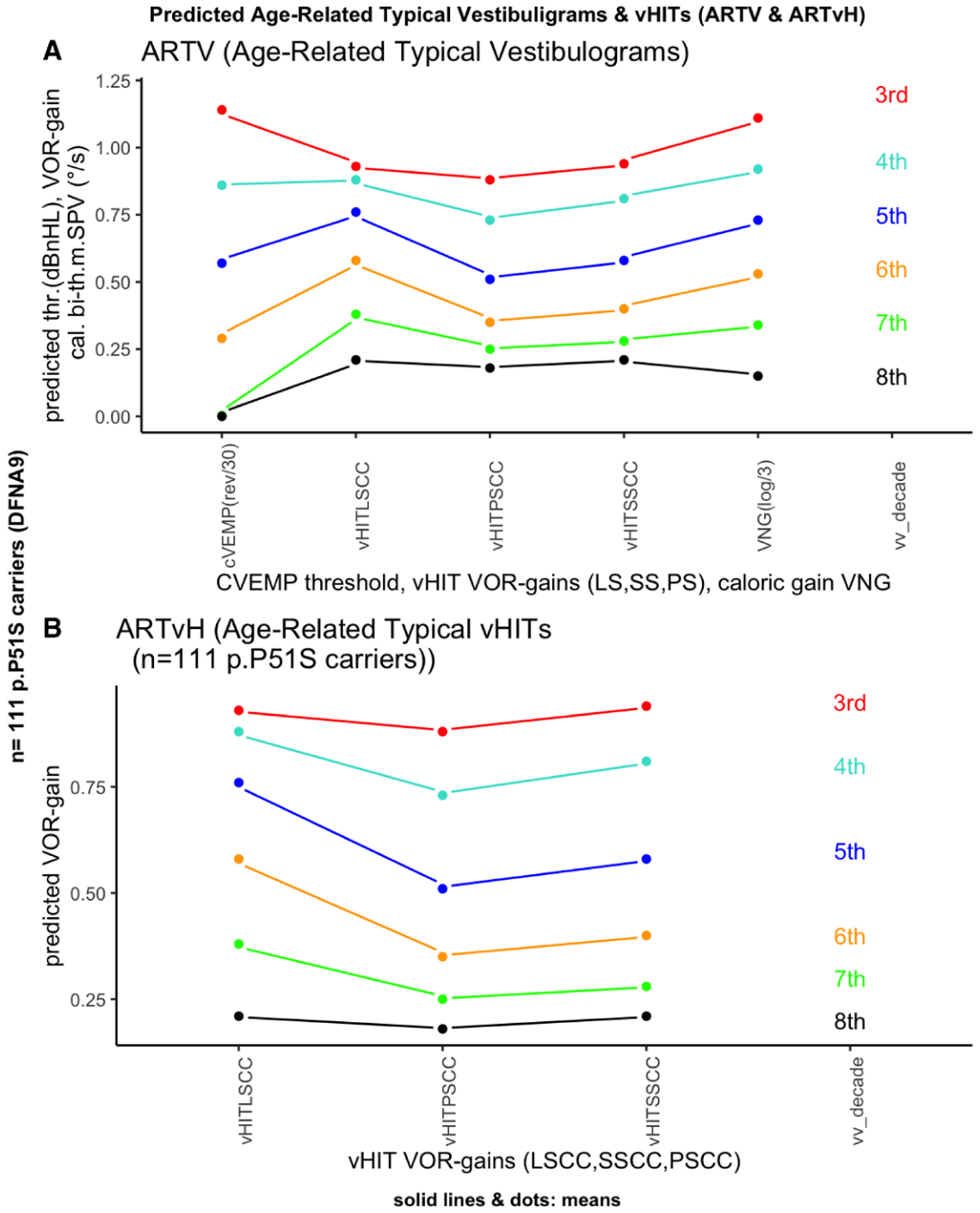

Fig. 8. Age-related typical vestibulograms (ARTV) and age-related typical vHITs (ARTvH) with predicted values obtained by modeling vestibular test results (C-VEMP thresholds (dBnHL), caloric bi-thermal maximal peak SPV gain and vHIT VOR-gains of the three SCCs (LSCC, SSCC, PSCC), after fitting regression models. A, ARTV. B, ARTvHI. LSCC, lateral semicircular canal; PSCC, posterior semicircular canal; SSCC, superior semicircular canal.

which regression models fitted the data, despite optimal transformations of data and of type of regression. The caloric function deteriorated early and reached levels that were beyond limits of areflexia as defined by the Barany Society criteria for BVP in the 6th decade.

Because vHIT VOR-gains were not different between both the centers, caloric test using air stimulation paradigm was probably less sensitive and yielded higher risk of false-positive results. The authors therefore focused on responses from water stimulation. Another reason is that Barany criteria were defined only for caloric SPV elicited with water irrigation as a stimulus. Hence, air irrigation gives completely different caloric SPV, with large differences in amplitude, which are not attributable to patient population, which means that Barany criteria of less than 6°/s are not applicable to caloric SPV with air irrigation as a stimulus. Caloric responses using air stimulation as a stimulus needs specific definitions and criteria for defining BVP, for instance a cutoff limit of 10°/s with air irrigation at 25°C and

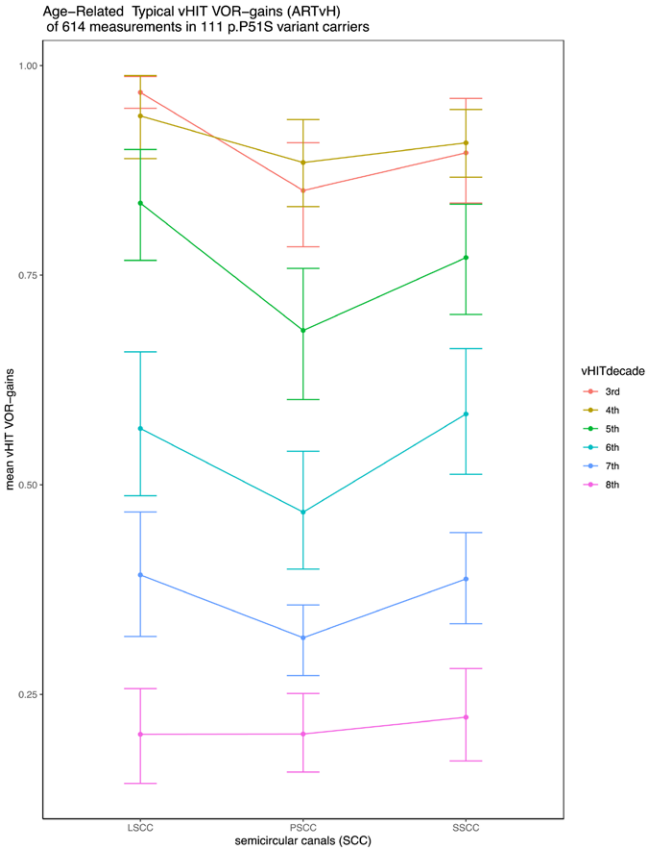

Fig. 9. Age-related typical vHIT VOR-gains (ARTvH) (means and 95% confidence intervals) n = 111 p.P51S variant carriers.

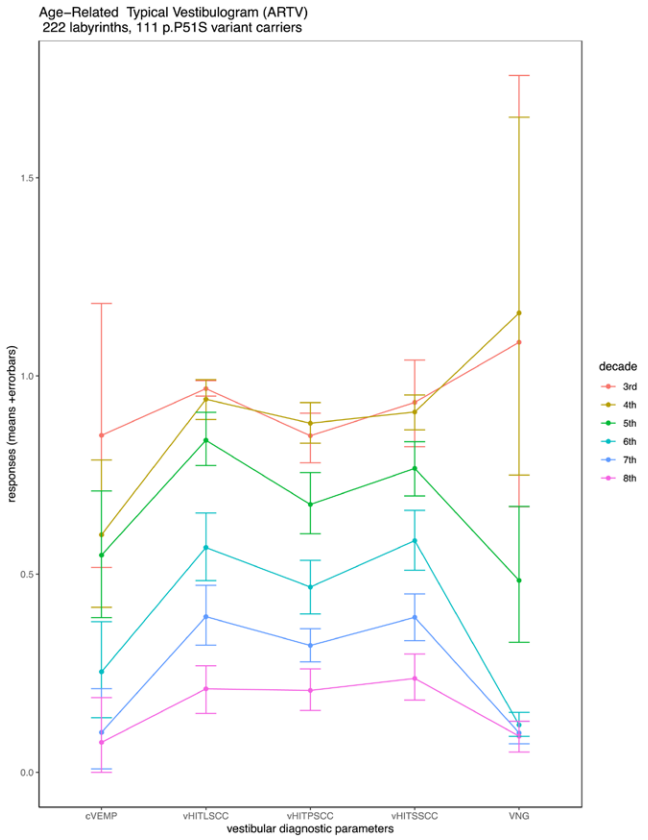

Fig. 10. Age-related typical observed vestibulograms (ARTV), based in measurements. To obtain optimal visualization, c-VEMP thresholds were reversed and rescaled with factor (1/30), caloric bi-thermal maximal peak SPV values were rescaled with factor (1/30) (means+95% confidence intervals). SPV, slow-phase velocity.

44°C for a duration of 60 seconds (van de Berg et al. 2020). The results of caloric responses elicited with air irrigation were nevertheless presented in the tables and figures for completeness but must be assessed with the necessary nuance.

In contrast, both estimates and visually enforced determination of the age of onset were consistent for all vHIT VOR-gains (Figs. 2, 3, and 8, Table 2). Baseline offset vHIT VOR-gain values of both vertical canals were relatively lower compared with those of the lateral (horizontal), which is consistent with the literature (McGarvie et al. 2015).

The vHIT VOR-gains remained stable for a prolonged time span compared to the caloric and vestibular myogenic evoked responses, however, with similar deterioration sequence as observed in previous studies reporting on vHIT VOR-gains in BVP caused by other etiologies. (Tarnutzer et al. 2016, 2017, 2018) The PSCC was the first to decline (5th decade), followed by the SSCC and the LSCC (6th decade).

As summarized in Table 2, hearing loss at 6 and 8 kHz in female carriers was estimated to start at about 35 and 28 years on average, respectively, which is before the start of caloric gain deterioration (estimation: 37 years, visual start: 45–49 years; 5th decade). For male carriers, hearing loss at highest frequencies was estimated at about 45 to 48 years on average. In Figure 11, the auditory function (at all hearing frequencies in male carriers, and the majority of hearing frequencies except for 6 and 8 kHz for their female peers) accelerated in a short time span between 40 and 50 years. Also, caloric bi-thermal maximal peak SPV deterioration preceded that of hearing decline with almost 9 years for male, and with about 5 years for female carriers. This seems to correspond with the estimated 9 years by Bischoff et al. (2005), who postulated that vestibular function would precede the hearing deterioration with a similar interval. These findings result from estimations, whereas different conclusions can be drawn with observed data and categorical approach, as shown in Tables 6 and 7. Common findings are that C-VEMP responses are the earliest to show signs of decline, together with hearing function at 6 and 8 kHz in female carriers (3rd decade), whereas the VOR-gains of the SSCC and the LSCC only start to deteriorate in the 6th decade. Both approaches have also in common that vHIT VOR-gain at the PSCC are the first to decline in comparison with the

TABLE 5. Chronological onset of dysfunction of different vestibular end-organs according to one-sample t test (+: mμ = significantly greater or less than the corresponding age-referenced limit)

Decade	VNG water	VNG air	vHIT LSCC	vHIT SSCC	vHIT PSCC	vHIT av. 3 SCC	C-VEMP
3rd	–	–	–	–	–	–	+
4th	–	+	–	–	–	–	+
5th	+	+	-	-	+	–	+
6th	+	+	+	+	+	+	+
7th	+	+	+	+	+	+	+

LSCC, lateral semicircular canal; PSCC, posterior semicircular canal; SSCC, superior semicircular canal; VEMP, vestibular-evoked myogenic evoked potentials; vHIT, the video Head Impulse Test; VNG, videonystagmography.

TABLE 6. Chronology of auditory and vestibular functional deterioration, based on estimates (regression)

Onset Number	End-Organ	Location/Frequency	Age (yrs)
#1	Vestibular Organ	Lateral SCC* Caloric Stimulation (VNG Air)	26.09 (Air Irrigation)
#2	Cochlea	8 kHz	27.85 (female carriers)
#3	Vestibular organ	Otolith (sacculus)	31.39
#4	Cochlea	PTA 6–8 kHz	31.79 (female carriers)
#5	Cochlea	6 kHz	34.92 (female carriers)
#6	Cochlea	PTA 4–8 kHz	35.60 (female carriers)
#7	Vestibular organ	Lateral SCC caloric stimulation (VNG water)	36.40 (water irrigation)
#8	Cochlea	4 kHz	37.69 (female carriers)
#9	Cochlea	0.250 kHz	38.62 (female carriers)
#10	Cochlea	PTA 0.5–4 kHz	40.85 (female carriers)
#11	Cochlea	2 kHz	41.66 (female carriers)
#12	Cochlea	0.500 kHz	41.80 (female carriers)
#13	Cochlea	2 kHz	41.93 (male carriers)
#14	Cochlea	1 kHz	42.13 (female carriers)
#15	Cochlea	0.125 kHz	42.86 (female carriers)
#16	Cochlea	0.500 kHz	44.62 (male carriers)
#17	Cochlea	0.250 kHz	44.66 (male carriers)
#18	Cochlea	0.125 kHz	44.98 (male carriers)
#19	Cochlea	4 kHz	45.68 (male carriers)
#20	Cochlea	PTA 0.5–4 kHz	45.85 (male carriers)
#21	Cochlea	1 kHz	46.45 (male carriers)
#22	Vestibular organ	Posterior SCC vHIT VOR	47.5
#23	Cochlea	PTA 4–8 kHz	47.72 (male carriers)
#24	Cochlea	6 kHz	48.55 (male carriers)
#25	Cochlea	8 kHz	48.60 (male carriers)
#26	Cochlea	PTA 6–8 kHz	49.42 (male carriers)
#27	Vestibular organ	Lateral SCC vHIT VOR	51.79
#28	Vestibular organ	Superior SCC vHIT VOR	56.65

PTA, pure-tone average; SPV, slow-phase velocity; SCC, semicircular canal; vHIT, the video Head Impulse Test; VOR, vestibulo-ocular reflex; VNG, videonystagmography.

TABLE 7. Deterioration sequence of main auditory and vestibular function decline according to visual determination of age of onset

Vestibular End Organ	Decade of Onset
Otolith: sacculus (C-VEMP)	3rd
Caloric gain LSCC (water)	5th
Caloric gain LSCC (air)	4th
vHIT LSCC	6th
vHIT SSCC	6th
vHIT PSCC	5th
PTA 0.5–4 kHz male	5th
PTA 0.5–4 kHz female	5th
PTA 4–8 kHz male	5th
PTA 4–8 kHz female	3rd
PTA 6–8 kHz male	5th
PTA 6–8 kHz female	3rd

LSCC, lateral semicircular canal; PSCC, posterior semicircular canal; PTA, pure tone average; SSCC, superior semicircular canal; VEMP, vestibular-evoked myogenic evoked potentials; vHIT, the video Head Impulse Test; VNG, videonystagmography.

other two SCCs and that the majority of hearing function begins to deteriorate in the 5th decade, regardless of gender.

In the past, vestibular function was mainly studied in p.P51S variant carriers using the velocity step test administered on a rotatory chair (Bischoff et al. 2005). The Time-constant (T) is a measure of the time needed for the nystagmus elicited during the high-speed angular acceleration, to decrease to 63% of its initial amplitude (Theunissen et al. 1988). The Time-constant (T) only reflects the function of the LSCC (horizontal) SCC. Remarkably, even though LSCC function tests are carried out with completely different frequencies, caloric stimulation and mid-high angular (100°/s) velocity step test generate similar results (an average age of onset of 34–36 years [4th decade]) but that was much different from higher angular tests, such as vHIT tests (at level of LSCC) (150–300°/s, 3–5 Hz) (6th decade).

Figure 6 illustrated that about 35% of the p.P51S variant carriers with caloric bi-thermal 30°C to 44°C sum of maximal peak SPV values under 6°/s (which is the cutoff value proposed by the Barany Society for BVP) still presented vHIT VOR-gains that were presumed normal (VOR-gain above 0.8). This was especially the case with water irrigation as a stimulus. This finding also leads to the hypothesis of "conductive" versus "sensorineural" vestibulopathy. Caloric responses are based upon a nonphysiologic stimulus, causing a deflection of the cupula of a verticalized horizontal canal only by very slow velocity caloric convection, whereas the head impulse is based upon a high-frequency physiologic stimulus, causing a more pronounced cupula deflection, or at least, this deflection might survive less optimal endolymphatic conditions in opposition to the nonphysiologic stimulation (Iversen & Rabbitt 2017; Muller 2020). We put forward the hypothesis that those p.P51S carriers presenting relatively normal vHIT VOR-gains with highly reduced caloric responses (bi-thermal maximal peak SPV < 6°/s) may present so-called conductive vestibulopathy due to restriction of the convective properties of the canal, before secondary "neurosensorial" vestibulopathy when vHIT VOR-gains drop to minimal values, for example, when dendritic cellular loss occurs due to extracellular deposition of misfolded mutant cochlin. This may coincide with our previous reports on radiological lesions in DFNA9 disease caused by the P.P51S variant in *COCH*, consisting of focal sclerosis and narrowing of one or more SCC in advanced stages of the disease, with the PSCC as the most frequent site of these lesions, which are observed in more than 90% of the carriers aged 49 or older (de Varebeke et al. 2014). Whether this may also explain the fact that PSCC vHIT VOR-gains are declining first, remains to be explored. This conductive/neurosensorial theory, however, is based on the assumption that caloric response is elicited almost exclusively by cupula deflection due to caloric convection and not exclusively by thermal excitation of the hair cells (Zucca et al. 1999).

There seems to be a relationship between the presence of O-VEMP and C-VEMP signal and a younger age, better auditory, and vestibular function. The younger the patient is, the better the hearing and the better the vestibular function, the better the chance of detecting C- and O-VEMP responses. Hence, C-VEMPs seemed to deteriorate at very early stages and responses were lost very quickly with aging. This may be another argument in favor of vestibular function preceding the hearing deterioration.

In contrast, vHIT VOR-gains were estimated to be the last to start signs of decline, approximately 18 years after VEMPs, 13 years after caloric bi-thermal maximal peak SPV, and up to 25 years after high-frequency hearing decline in female carriers.

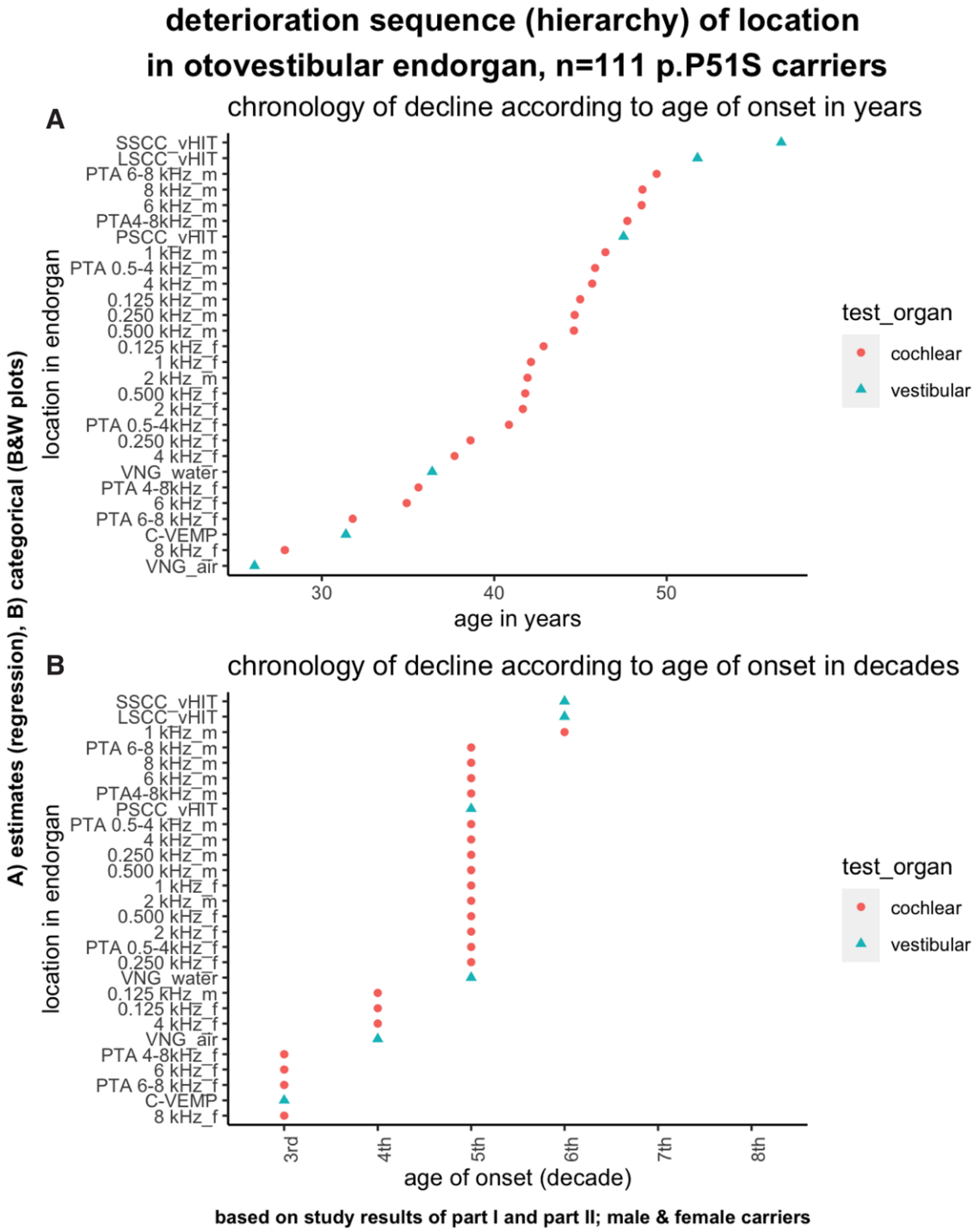

Fig. 11. Decline hierarchy of both auditory and vestibular dysfunction: location of end-organ versus age of onset (years). Note the "_f" refers to female and "_m" refers to male for the hearing frequencies.

Limitations

In this study, O-VEMP tests were administered to a limited number of p.P51S variant carriers (30 out of 111, or 27% of subjects). Furthermore, different caloric stimulations were used in both centers (water versus air irrigation). Because bi-thermal maximal peak SPV values were significantly different between both caloric stimulation methods in term of amplitude and decrease rate, these could not be analyzed as one and we concentrated on SPV values elicited with water irrigation as a stimulus.

The definition of hyporeflexia and areflexia or vestibular dysfunction is not always straightforward with regard to relatively new diagnostic tools, such as C-VEMPs and vHIT tests, however, especially for VNG caloric SPV elicited with air irrigation. Since Barany criteria for areflexia were only defined for water irrigation as a stimulus, those for air irrigation are unavailable and probably different from the 6°/s limit. Also, different parameters could be applied to vHIT VOR-gain values to define abnormal function, such as those defined for presbyvestibulopathy,

which are different from the criteria for BVP. Moreover, the frequency or numbers of corrective saccades may have important additional value in the interpretation of vHIT results, which will probably be adjusted in the future (Janky et al. 2018). For these reasons, we only focused on gain values in accordance with the Barany Society criteria for BVP.

CONCLUSION

The first signs of the vestibular function decline in DFNA9 patients, caused by the p.P51S variant in *COCH*, occur with C-VEMP activity (3rd decade), followed by deterioration of caloric responses and vHIT VOR-gains of the PSCC (4th–5th decade). The other two SCCs (SSCC and LSCC) conclude with late-onset decay in the 6th decade. These findings emphasize the need to expand vestibular function evaluation to all SCC and otolith organs as well as using a test battery that covers a more comprehensive range of frequency spectrum of the vestibular sensory organ.

To further refine the present findings, a prospective longitudinal study of the auditory and vestibular phenotype may help to provide even better insights in this matter.

ACKNOWLEDGMENTS

The authors would like to thank the Dutch-Belgian DFNA9patient association "De negende van" for their support in recruiting patients.

S.J., V.V.R., and J.M. selected and identified all family pedigrees and enrolled participants to the study each at both centers (Hasselt and Antwerp, Belgium). J.M., B.B., K.D., and C.N. administered clinical audiometric investigations. All vestibular data at the Hasselt center were administered by S.J., whereas these were done by J.M. at the Antwerp center. S.J. and J.M. reviewed data from all sites. All descriptive and inferential statistics were conducted by S.J. and corrected as well as supervised by E.F. Molecular analysis was conducted by G.V.C. The manuscript and Supplemental Digital Content, http://links.lww.com/EANDH/A821, were written by S.J. All revisions were carried out by S.J. and E.F. All authors discussed the results and implications and commented on the manuscript at all stages. The project was supervised by V.V.R. and O.V.V.

The authors have no conflicts of interest to disclose.

Address for correspondence: Sebastien P. F. JanssensdeVarebeke, Department of Otorhinolaryngology, Jessa Hospital, Stadsomvaart 11, 3500 Hasselt, Belgium. E-mail: drsjanssens@gmail.com

Received March 30, 2020; accepted March 31, 2021; published online ahead of print August 6, 2021.

REFERENCES

Agrawal, Y., Pineault, K. G., Semenov, Y. R. (2018). Health-related quality of life and economic burden of vestibular loss in older adults. *Laryngoscope Investig Otolaryngol, 3*, 8–15.

Bae, S. H., Robertson, N. G., Cho, H. J., Morton, C. C., Jung, D. J., Baek, J. I., Choi, S. Y., Lee, J., Lee, K. Y., Kim, U. K. (2014). Identification of pathogenic mechanisms of COCH mutations, abolished cochlin secretion, and intracellular aggregate formation: Genotype-phenotype correlations in DFNA9 deafness and vestibular disorder. *Hum Mutat, 35*, 1506–1513.

Bischoff, A. M., Huygen, P. L., Kemperman, M. H., Pennings, R. J., Bom, S. J., Verhagen, W. I., Admiraal, R. J., Kremer, H., Cremers, C. W. (2005). Vestibular deterioration precedes hearing deterioration in the P51S COCH mutation (DFNA9): An analysis in 74 mutation carriers. *Otol Neurotol, 26*, 918–925.

Bom, S. J., Kemperman, M. H., De Kok, Y. J., Huygen, P. L., Verhagen, W. I., Cremers, F. P., Cremers, C. W. (1999). Progressive cochleovestibular impairment caused by a point mutation in the COCH gene at DFNA9. *Laryngoscope, 109*, 1525–1530.

Bom, S. J., Kemperman, M. H., Huygen, P. L., Luijendijk, M. W., Cremers, C. W. (2003). Cross-sectional analysis of hearing threshold in relation to age in a large family with cochleovestibular impairment thoroughly genotyped for DFNA9/COCH. *Ann Otol Rhinol Laryngol, 112*, 280–286.

Booth, K. T., Ghaffar, A., Rashid, M., Hovey, L. T., Hussain, M., Frees, K., Renkes, E. M., Nishimura, C. J., Shahzad, M., Smith, R. J., Ahmed, Z., Azaiez, H., Riazuddin, S. (2020). Novel loss-of-function mutations in COCH cause autosomal recessive nonsyndromic hearing loss. *Hum Genet, 139*, 1565–1574.

Curthoys, I. S. (2010). A critical review of the neurophysiological evidence underlying clinical vestibular testing using sound, vibration and galvanic stimuli. *Clin Neurophysiol*, *121*, 132–144.

Curthoys, I. S., Vulovic, V., Manzari, L. (2012). Ocular vestibular-evoked myogenic potential (oVEMP) to test utricular function: Neural and oculomotor evidence. *Acta Otorhinolaryngol Ital, 32*, 41–45.

Dale, O., Salo, M. (1996). The helsinki declaration, research guidelines and regulations: Present and future editorial aspects. *Acta Anaesthesiol Scand, 40*, 771–772.

de Kok, Y. J., Bom, S. J., Brunt, T. M., Kemperman, M. H., van Beusekom, E., van der Velde-Visser, S. D., Robertson, N. G., Morton, C. C., Huygen, P. L., Verhagen, W. I., Brunner, H. G., Cremers, C. W., Cremers, F. P. (1999). A Pro51Ser mutation in the COCH gene is associated with late onset autosomal dominant progressive sensorineural hearing loss with vestibular defects. *Hum Mol Genet, 8*, 361–366.

de Varebeke, S. P., Termote, B., Van Camp, G., Govaerts, P. J., Schepers, S., Cox, T., Deben, K., Ketelslagers, K., Souverijns, G. (2014). Focal sclerosis of semicircular canals with severe DFNA9 hearing impairment caused by a P51S COCH-mutation: Is there a link? *Otol Neurotol, 35*, 1077–1086.

Dobbels, B., Peetermans, O., Boon, B., Mertens, G., Van de Heyning, P., Van Rompaey, V. (2019). Impact of bilateral vestibulopathy on spatial and nonspatial cognition: A systematic review. *Ear Hear, 40*, 757–765.

Downie, L., Halliday, J., Burt, R., Lunke, S., Lynch, E., Martyn, M., Poulakis, Z., Gaff, C., Sung, V., Wake, M., Hunter, M. F., Saunders, K., Rose, E., Lewis, S., Jarmolowicz, A., Phelan, D., Rehm, H. L., Amor, D. J.; Melbourne Genomics Health Alliance. (2020). Exome sequencing in infants with congenital hearing impairment: A population-based cohort study. *Eur J Hum Genet, 28*, 587–596.

Eppsteiner, R. W., Smith, R. J. (2011). Genetic disorders of the vestibular system. *Curr Opin Otolaryngol Head Neck Surg, 19*, 397–402.

Fransen, E., Van Camp, G. (1999). The COCH gene: A frequent cause of hearing impairment and vestibular dysfunction? *Br J Audiol, 33*, 297–302.

Guinand, N., Boselie, F., Guyot, J. P., Kingma, H. (2012). Quality of life of patients with bilateral vestibulopathy. *Ann Otol Rhinol Laryngol, 121*, 471–477.

Halmagyi, G. M., Chen, L., MacDougall, H. G., Weber, K. P., McGarvie, L. A., Curthoys, I. S. (2017). The video Head Impulse Test. *Front Neurol, 8*, 258.

Hermann, R., Ionescu, E. C., Dumas, O., Tringali, S., Truy, E., Tilikete, C. (2018). Bilateral vestibulopathy: Vestibular function, dynamic visual acuity and functional impact. *Front Neurol, 9*, 555.

Ikezono, T., Omori, A., Ichinose, S., Pawankar, R., Watanabe, A., Yagi, T. (2001). Identification of the protein product of the Coch gene (hereditary deafness gene) as the major component of bovine inner ear protein. *Biochim Biophys Acta, 1535*, 258–265.

Iversen, M. M., Rabbitt, R. D. (2017). Wave mechanics of the vestibular semicircular canals. *Biophys J, 113*, 1133–1149.

Janky, K. L., Patterson, J., Shepard, N., Thomas, M., Barin, K., Creutz, T., Schmid, K., Honaker, J. A. (2018). Video Head Impulse Test (vHIT): The role of corrective saccades in identifying patients with vestibular loss. *Otol Neurotol, 39*, 467–473.

JanssensdeVarebeke, S. P. F., Van Camp, G., Peeters, N., Elinck, E., Widdershoven, J., Cox, T., Deben, K., Ketelslagers, K., Crins, T., Wuyts, W. (2018). Bi-allelic inactivating variants in the COCH gene cause autosomal recessive prelingual hearing impairment. *Eur J Hum Genet, 26*, 587–591.

Khetarpal, U. (2000). DFNA9 is a progressive audiovestibular dysfunction with a microfibrillar deposit in the inner ear. *Laryngoscope, 110*, 1379–1384.

Kim, S., Oh, Y. M., Koo, J. W., Kim, J. S. (2011). Bilateral vestibulopathy: Clinical characteristics and diagnostic criteria. *Otol Neurotol, 32*, 812–817.

Lemaire, F. X., Feenstra, L., Huygen, P. L., Fransen, E., Devriendt, K., Van Camp, G., Vantrappen, G., Cremers, C. W., Wackym, P. A., Koss, J. C. (2003). Progressive late-onset sensorineural hearing loss and vestibular impairment with vertigo (DFNA9/COCH): Longitudinal analyses in a belgian family. *Otol Neurotol, 24*, 743–748.

Lucieer, F., Vonk, P., Guinand, N., Stokroos, R., Kingma, H., van de Berg, R. (2016). Bilateral vestibular hypofunction: Insights in etiologies, clinical subtypes, and diagnostics. *Front Neurol, 7*, 26.

Lucieer, F. M. P., Van Hecke, R., van Stiphout, L., Duijn, S., Perez-Fornos, A., Guinand, N., Van Rompaey, V., Kingma, H., Joore, M., van de Berg, R. (2020). Bilateral vestibulopathy: Beyond imbalance and oscillopsia. *J Neurol, 267*(Suppl 1), 241–255.

Maes, L., Dhooge, I., D'haenens, W., Bockstael, A., Keppler, H., Philips, B., Swinnen, F., Vinck, B. M. (2010). The effect of age on the sinusoidal harmonic acceleration test, pseudorandom rotation test, velocity step test, caloric test, and vestibular-evoked myogenic potential test. *Ear Hear, 31*, 84–94.

Manolis, E. N., Yandavi, N., Nadol, J. B. Jr, Eavey, R. D., McKenna, M., Rosenbaum, S., Khetarpal, U., Halpin, C., Merchant, S. N., Duyk, G. M., MacRae, C., Seidman, C. E., Seidman, J. G. (1996). A gene for non-syndromic autosomal dominant progressive postlingual sensorineural hearing loss maps to chromosome 14q12-13. *Hum Mol Genet, 5*, 1047–1050.

McGarvie, L. A., MacDougall, H. G., Halmagyi, G. M., Burgess, A. M., Weber, K. P., Curthoys, I. S. (2015). The video Head Impulse Test (vHIT) of semicircular canal function - Age-Dependent normative values of VOR gain in healthy subjects. *Front Neurol, 6*, 154.

Muller, M. (2020). Mechanical aspects of the semicircular ducts in the vestibular system. *Biol Cybern*, *114*, 421–442.

Rinne, T., Bronstein, A. M., Rudge, P., Gresty, M. A., Luxon, L. M. (1998). Bilateral loss of vestibular function: Clinical findings in 53 patients. *J Neurol, 245*, 314–321.

Robertson, N. G., Hamaker, S. A., Patriub, V., Aster, J. C., Morton, C. C. (2003). Subcellular localisation, secretion, and post-translational processing of normal cochlin, and of mutants causing the sensorineural deafness and vestibular disorder, DFNA9. *J Med Genet, 40*, 479–486.

Robertson, N. G., Khetarpal, U., Gutiérrez-Espeleta, G. A., Bieber, F. R., Morton, C. C. (1994). Isolation of novel and known genes from a human fetal cochlear cDNA library using subtractive hybridization and differential screening. *Genomics, 23*, 42–50.

Robertson, N. G., Lu, L., Heller, S., Merchant, S. N., Eavey, R. D., McKenna, M., Nadol, J. B. Jr, Miyamoto, R. T., Linthicum, F. H. Jr, Lubianca Neto, J. F., Hudspeth, A. J., Seidman, C. E., Morton, C. C., Seidman, J. G. (1998). Mutations in a novel cochlear gene cause DFNA9, a human nonsyndromic deafness with vestibular dysfunction. *Nat Genet, 20*, 299–303.

Robertson, N. G., Resendes, B. L., Lin, J. S., Lee, C., Aster, J. C., Adams, J. C., Morton, C. C. (2001). Inner ear localization of mRNA and protein products of COCH, mutated in the sensorineural deafness and vestibular disorder, DFNA9. *Hum Mol Genet, 10*, 2493–2500.

Robertson, N. G., Skvorak, A. B., Yin, Y., Weremowicz, S., Johnson, K. R., Kovatch, K. A., Battey, J. F., Bieber, F. R., Morton, C. C. (1997). Mapping and characterization of a novel cochlear gene in human and in mouse: A positional candidate gene for a deafness disorder, DFNA9. *Genomics, 46*, 345–354.

Strupp, M., Kim, J. S., Murofushi, T., Straumann, D., Jen, J. C., Rosengren, S. M., Della Santina, C. C., Kingma, H. (2017). Bilateral vestibulopathy: Diagnostic criteria consensus document of the classification Committee of the Bárány Society. *J Vestib Res, 27*, 177–189.

Sun, D. Q., Ward, B. K., Semenov, Y. R., Carey, J. P., Della Santina, C. C. (2014). Bilateral vestibular deficiency: Quality of life and economic implications. *JAMA Otolaryngol Head Neck Surg, 140*, 527–534.

Tarnutzer, A. A., Bockisch, C. J., Buffone, E., Weber, K. P. (2017). Association of posterior semicircular canal hypofunction on video-head-impulse testing with other vestibulo-cochlear deficits. *Clin Neurophysiol, 128*, 1532–1541.

Tarnutzer, A. A., Bockisch, C. J., Buffone, E., Weber, K. P. (2018). Hierarchical cluster analysis of semicircular canal and otolith deficits in bilateral vestibulopathy. *Front Neurol, 9*, 244.

Tarnutzer, A. A., Bockisch, C. J., Buffone, E., Weiler, S., Bachmann, L. M., Weber, K. P. (2016). Disease-specific sparing of the anterior semicircular canals in bilateral vestibulopathy. *Clin Neurophysiol, 127*, 2791–2801.

Theunissen, E. J., Huygen, P. L., Folgering, H. T., Nicolasen, M. G. (1988). The velocity step test. Its use in the evaluation of the effects of drugs in dizzy patients. *Acta Otolaryngol Suppl, 460*, 104–113.

van de Berg, R., Ramos, A., van Rompaey, V., Bisdorff, A., Perez-Fornos, A., Rubinstein, J. T., Phillips, J. O., Strupp, M., Della Santina, C. C., Guinand, N. (2020). The vestibular implant: Opinion statement on implantation criteria for research. *J Vestib Res, 30*, 213–223.

Van Der Stappen, A., Wuyts, F. L., Van De Heyning, P. H. (2000). Computerized electronystagmography: Normative data revisited. *Acta Otolaryngol, 120*, 724–730.

Vanspauwen, R., Wuyts, F. L., Krijger, S., Maes, L. K. (2017). Comparison of different electrode configurations for the oVEMP with bone-conducted vibration. *Ear Hear, 38*, 205–211.

Verhagen, W. I., Huygen, P. L., Joosten, E. M. (1988). Familial progressive vestibulocochlear dysfunction. *Arch Neurol, 45*, 766–768.

Verstreken, M., Declau, F., Wuyts, F. L., D'Haese, P., Van Camp, G., Fransen, E., Van den Hauwe, L., Buyle, S., Smets, R. E., Feenstra, L., Van der Stappen, A., Van de Heyning, P. H. (2001). Hereditary otovestibular dysfunction and Ménière's disease in a large Belgian family is caused by a missense mutation in the COCH gene. *Otol Neurotol, 22*, 874–881.

Wuyts, F. L., Furman, J., Vanspauwen, R., Van de Heyning, P. (2007). Vestibular function testing. *Curr Opin Neurol, 20*, 19–24.

Zingler, V. C., Cnyrim, C., Jahn, K., Weintz, E., Fernbacher, J., Frenzel, C., Brandt, T., Strupp, M. (2007). Causative factors and epidemiology of bilateral vestibulopathy in 255 patients. *Ann Neurol, 61*, 524–532.

Zucca, G., Botta, L., Valli, S., Giannoni, B., Mira, E., Perin, P., Valli, P. (1999). Caloric stimulation of ampullar receptors: A new method to produce mechanically-evoked responses in frog semicircular canals. *J Neurosci Methods, 88*, 141–151.